EUROPEAN COMMISSION

Community Research

SEVENTH FRAMEWORK PROGRAMME

CARBOWASTE

Treatment and Disposal of Irradiated Graphite and Other Carbonaceous Waste

Grant Agreement Number: FP7-211333



- Technical Report (WP 6 Task 1) –

- WATER IMPREGNATION KINETICS IN NUCLEAR GRAPHITE SAMPLES FROM UNGG REACTORS -

Author(s): **J. COMTE – C. GUY**

Date of issue of this report : November 2010

Start date of project : **01/04/2008** Duration : **48 Months**

Project co-funded by the European Commission under the Seventh Framework Programme (2007 to 2011) of the European Atomic Energy Community (EURATOM) for nuclear research and training activities		
Dissemination Level		
PU	Public	
RE	Restricted to the partners of the CARBOWASTE project	
CO	Confidential, only for specific distribution list defined on this document	**X**

Distribution list

Person and organisation name and/or group	Comments
W. Von Lensa, CARBOWASTE Project coordinator	
G. PINA, Work Package 3 leader	
B. Grambow, Work Package 6 leader	
L. Petit, EDF	
S. Schumacher, ANDRA	
M. Firon, CEA	
C. Ferry, CEA	
P. Thouvenot, CEA	
CARBOWASTE beneficiaries.	

CARBOWASTE		
Work package: 6 **Task: :** 6.1	**CARBOWASTE document no:** CARBOWASTE-1007-D-WP6.Task.1	**Document type: T** D=Deliverable / M=Minutes / P=Progress report / T=Technical Report
Issued by: CEA **Internal no.:** Technical report CEA water impregnation in UNGG graphite WP6		**Document status:** Final

Document title

WATER IMPREGNATION KINETICS IN NUCLEAR GRAPHITE SAMPLES FROM UNGG REACTORS

Executive summary

This document describes the experimental conditions and tests performed to measure the water impregnation kinetics in nuclear graphites. These tests were performed on non irradiated and irradiated graphite samples from the G2 and St Laurent A2 UNGG reactors.

The results show that water impregnation in non irradiated graphite from the G2 reactor is slow and low. The saturation rate only reached between 30% and 40% of the open porosity in samples after a period of 500 days. Water impregnation is faster and saturates practically all of the open porosity in samples of irradiated graphite.

A small difference in water impregnation is observed between the non irradiated and irradiated samples from the St Laurent A2 reactor, both in terms of their water impregnation kinetics and their porosity saturation rates.

Revisions

Rev.	Date	Short description	Author	Internal Review	Task Leader	WP Leader
		Issue	Name, Organisation	Name, Organisation Signature	Name, Organisation Signature	Name, Organisation Signature
00	7/12/2010	First issue	J. COMTE CEA	C. GUY CEA		B. Grambow SUBATECH

Table of Content

Introduction 5
Selection and preparation of samples 6
Summary of water impregnation in graphites 7
1.1. Immersion tests on fuel sleeve graphite samples 7
1.2. Immersion tests on stack graphite samples 10
1.3. Tests on Magnox-type graphite 11
1.4. Tests on Hanford graphite samples (USA) 12
1.5. Summary of data 13
Experimental measurements 13
G2 reactor 14
1.6. Sample preparation 14
1.6.1. G2 non-irradiated samples 14
1.6.2. G2 irradiated samples 15
1.7. Measurements on non irradiated graphite samples 18
1.8. Measurements on irradiated samples 20
1.9. Comparison of tests on G2 non irradiated and irradiated graphite samples 23
SLA2 reactor 24
1.10. Sample preparation 24
1.10.1. SLA2 non-irradiated samples 24
1.10.2. SLA2 irradiated samples 24
1.11. Measurements on non irradiated graphite samples 28
1.12. Measurements on irradiated graphite samples 29
1.13. Comparison of tests on St Laurent A2 non irradiated and irradiated graphite samples 32
Discussion 34
1.14. Kinetics and impregnation rate of non irradiated samples 34
1.15. Kinetics and impregnation rate of irradiated samples 38
1.16. Summary 46
Conclusion 47
LIST OF TABLES 48
LIST OF FIGURES 50

INTRODUCTION

Graphite was used as moderating material in UNGG reactors (graphite-moderated gas-cooled reactors fuelled with natural uranium) because of its mechanical, thermal and neutron properties.

In order to manage graphite waste disposal, it is necessary to collect data on the behaviour of the long-lived radionuclides ^{36}Cl and ^{14}C due to their mobility in the geological environment and their long radioactive half-lives.

An R&D program was developed to study and quantify the release mechanisms of these radionuclides in water. A state-of-the-art report has been drafted on the basis of available literature[1]. The release of radionuclides in solution depends on a number of physicochemical processes:

- Ingress of reagents (water) into radionuclide sites,
- Solubilisation of radionuclides,
- Transport of radionuclides in solution through graphite pores into the solution.

Analysis of the impregnation (impregnation speed, impregnation rate) of water in the porous graphite environment represents one of the main parameters that will greatly influence the physicochemical processes controlling the release of radionuclides in solution.

For this reason, the impregnation of samples from the G2 and St Laurent A2 (SLA2) reactors was studied in the *Laboratoire d'Analyses Radiochimiques et Chimiques* (DEC/SA3C/LARC) with support from the *Laboratoire d'Expertise et de Caractérisation Destructive* (DSN/SEEC/LECD). The samples had been characterised in a previous study by means of geometric density measurements, He pycnometry, Hg porosimetry, X-ray diffraction and Raman spectroscopy. The results are reported in a technical report[2].

The first part of this report provides a summary of the bibliographic information, as well as describing the measurement methodology and sample preparation.

The second part of this report discusses the impregnation measurements and the saturation rate calculations in relation to the sample characteristics.

SELECTION AND PREPARATION OF SAMPLES

Two different reactors – G2 and SLA2 – were investigated as part of the study on the behaviour of radionuclides in irradiated graphites in aqueous environments. These reactors were chosen due to the different characteristics of their stack graphite and their operating conditions, particularly:

- Type of coke and initial impurities,
- Neutron and thermal power levels, CO_2 pressure, thermal history of the graphite during reactor operation, and the presence of carboxyhydrogenated deposits.

Table 1 recalls the main differences between the G2 reactor and the SLA2 reactor. The choice of these two reactors can also be explained by the fact that there was a sufficient quantity of non-irradiated and irradiated graphite samples whose thermal and neutron histories were perfectly well-known.

Reactor	G2	SLA2
Divergence date	July 1958	June 1971
Shutdown date	February 1980	May 1992
Thermal power (MW)	260	1700
CO_2 pressure (MPa)	1.5	28.5
Mass of graphite stack (tonnes)	1,500	2,200
Graphite temperature during operation	140-380°C	240-470°C
Type of graphite (core)	Special A grade coke	MgF_2 cleaned lima coke
Carbonaceous deposits	Small	Large
Graphite density (g/cm^3)	1.71	1.684

TABLE 1: CHARACTERISTICS OF G2 AND SLA2 REACTORS

SUMMARY OF WATER IMPREGNATION IN GRAPHITES

There is little information in available literature on the study of water impregnation in nuclear-grade graphites. A few documents provide experimental data on graphites from the moderator and fuel sleeves of UNGG reactors.

1.1. Immersion tests on fuel sleeve graphite samples

Impregnation measurements were performed by AREVA NC in 2006 on non irradiated graphite samples taken from fuel sleeves [3]. The experimental protocol consisted in immersing sections or whole fuel sleeves at ambient temperature for a 3-month period and regularly monitoring their mass. Table 2 lists the characteristics of the graphite fuel sleeves.

Origin	Diameter (inner/outer)	Height	Mass	Density (g/cm^3)
Pechiney (batch 001499)	93/136 mm	460 mm	6,489.2 g	1,824
EDF batch St Laurent No. 17121953	111/137 mm	603 mm	5,245.1 g	1,696

TABLE 2: CHARACTERISATION OF SAMPLES

Figure 1 shows the variation in the water mass (in relation to the mass of the dry sample) impregnating the samples. It can be seen that this rate changes dramatically in relation to the size of the samples. When the size of the samples reduces, the kinetics and maximum impregnation rate at 90 days both increase: 7% for fragment sizes ranging between 33 and 55 mm compared with a rate of 28% for fragment sizes ranging between 1 and 4 mm. It must nevertheless be pointed out that though the mass of the thinnest fragments no longer changes after 40 days, a small variation can be observed in the rate for the biggest fragments and entire fuel sleeves. Fuel sleeves with the highest density show the lowest impregnation rate.

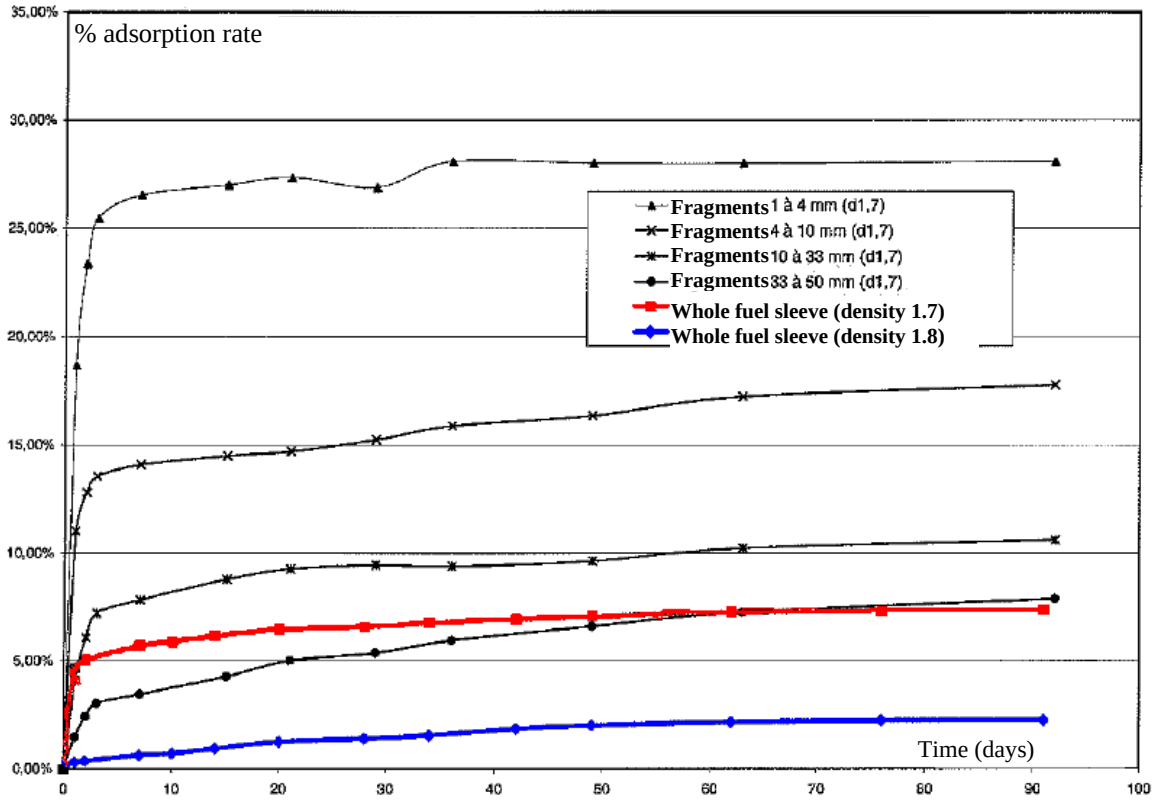


FIGURE 1: VARIATION IN THE QUANTITY OF WATER ADSORBED IN THE GRAPHITE SAMPLES

The authors did not calculate the impregnation rate of the samples in relation to closed porosity. However, based on the assumption of a total porosity of 23% which corresponds to a density of 1.7, the impregnation rate for the thinnest fragments is therefore higher than 100% (about 120%). This result points to the presence of a film of water on the outer surface of the samples, which leads to overestimating the impregnation rate all the more so since the surface-to-volume ratio of the samples is high. Table 3 lists the calculated impregnation rates at 90 days for the EDF fuel sleeve samples.

Sample	Impregnation rate at 90 days/ total porosity
1 – 4 mm fragments	#120%
4-10 mm fragments	#78%
10 – 33 mm fragments	#48%
33 – 50 mm fragments	#35%
whole fuel sleeve	#35%

TABLE 3: IMPREGNATION RATE OF EDF FUEL SLEEVE SAMPLES

The impregnation rate for the largest fragments and the entire fuel sleeve is about 35% at 90 days.
The data for the 10-33 mm fragment, 33-50 mm fragment and the entire fuel sleeve were recalculated and corrected in relation to the surface-to-volume ratio estimated on the basis of the geometries. It can be seen that the curves all look similar, which indicates that the impregnation kinetics follow a law that

is proportional to the V/S ratio. By applying a square-root-of-time rule to the data for the entire fuel sleeve, it can be seen that the kinetics follow a linear law that can be interpreted by a diffusion process.

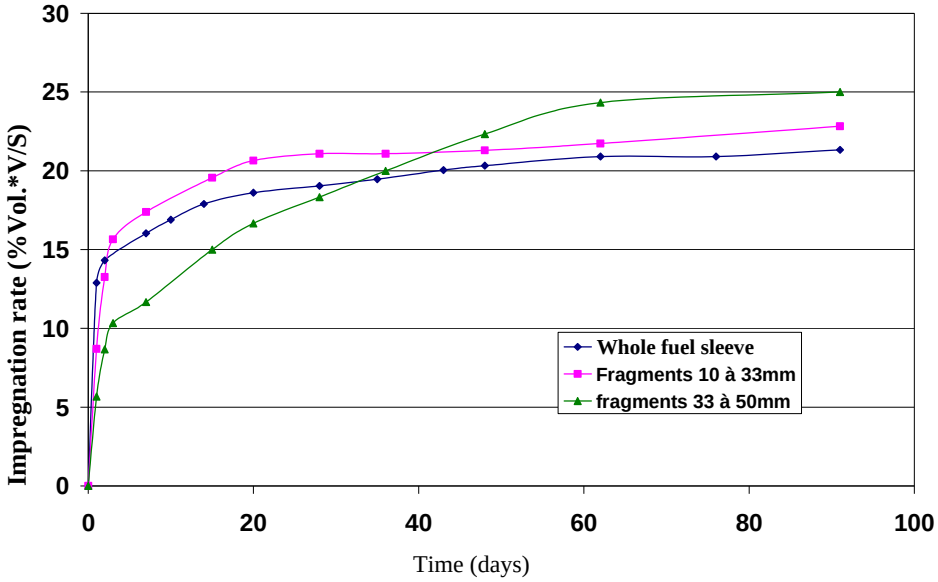


FIGURE 2: CORRECTED IMPREGNATION RATES OF THE V/S RATIO

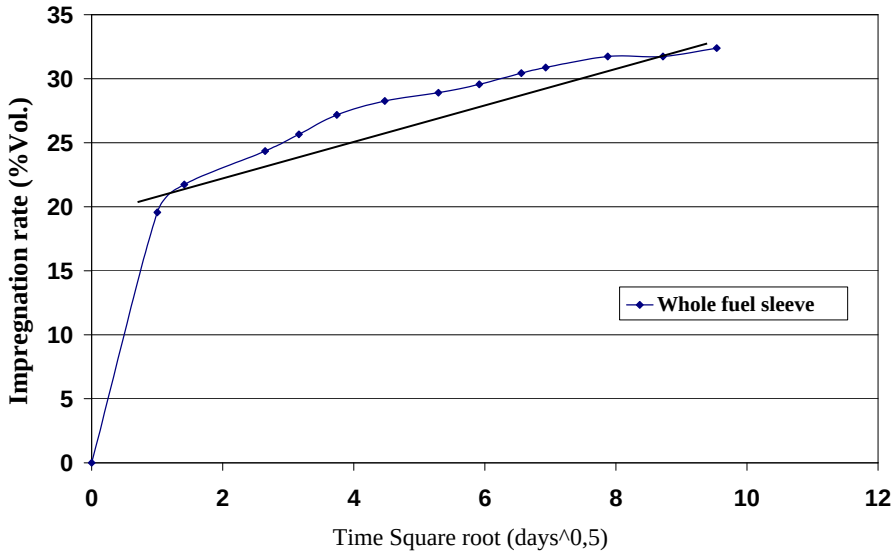


FIGURE 3: IMPREGNATION RATE VARIATIONS FOR THE ENTIRE FUEL SLEEVE USING THE SQUARE-ROOT-OF-TIME RULE

An AREVA NC document provides data on St Laurent graphite fuel sleeves which were stored in the reactor pool during decladding [4]. Irradiated and non-irradiated graphite samples were immersed in water for 24 hours under different pressure conditions. The mass gains are listed in Table 4.

	Irradiated sample (%)	Non-irradiated sample (%)
Atmospheric pressure	4.4	1.1
Atmospheric pressure + 1 bar	3.8	2.5

TABLE 4: MASS GAIN PERCENTAGES OF IRRAIDATED AND NON-IRRADIATED GRAPHITE SAMPLES

It is clear that the 24-hour period is insufficient for measuring the maximum impregnation rate, though this study seems to indicate that the impregnation rate is faster for irradiated samples.

1.2. Immersion tests on stack graphite samples

J.R. Costes *et al.* studied the conditioning of graphite bricks by impregnation in organic matrices (bitumen, epoxy resin) [5,6]. Their studies particularly focused on measuring the impregnation kinetics of water in two stack graphites: graphite from the G2 reactor and graphite from an unidentified UNGG reactor dubbed 'B'. The effect of the sample size and the oxidation rate by radiolytic corrosion was also studied. Figure 4 shows that the impregnation kinetics are relatively slow for G2 samples in relation to open porosity with a maximum saturation rate of 10% to 17% which is reached after 15 days. Figure 5 illustrates the effect of radiolytic corrosion which noticeably increases the kinetics and the maximum saturation rate. The most corroded sample shows a wear rate of 16.4%, having reached a 90% saturation rate after 25 days. Comparatively, non irradiated samples reached a saturation rate ranging between 35% and 50% over the same period. The authors explain this result by the fact that radiolytic corrosion increases the pore diameter which therefore facilitates water penetration.

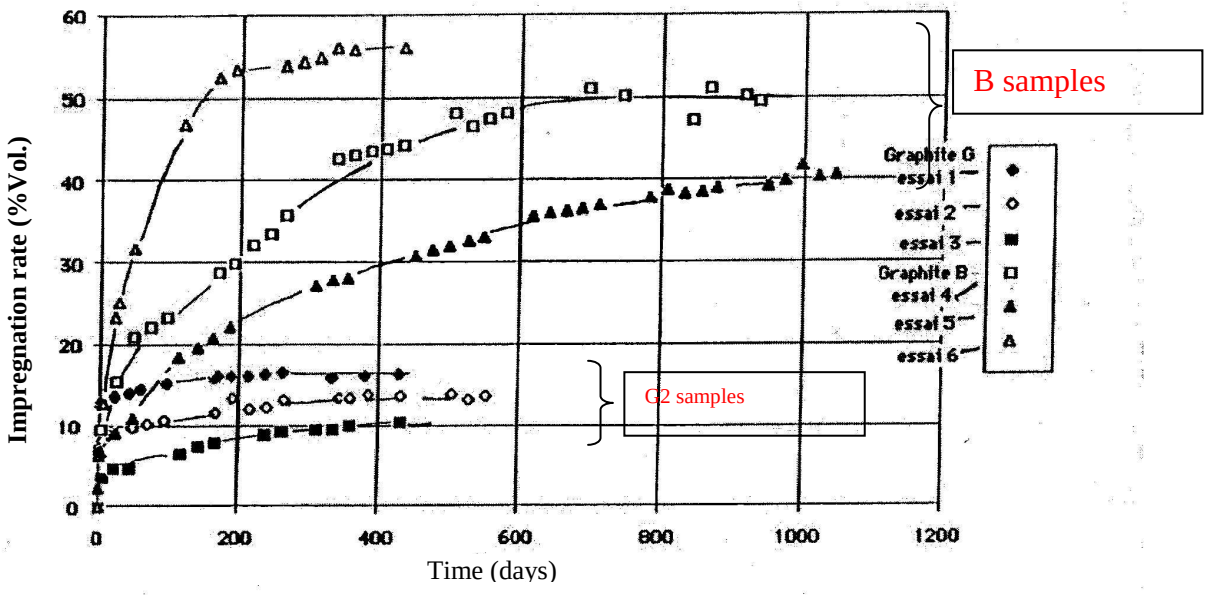


FIGURE 4: SATURATION RATE OF NON IRRADIATED SAMPLES FROM THE G2 AND B REACTORS

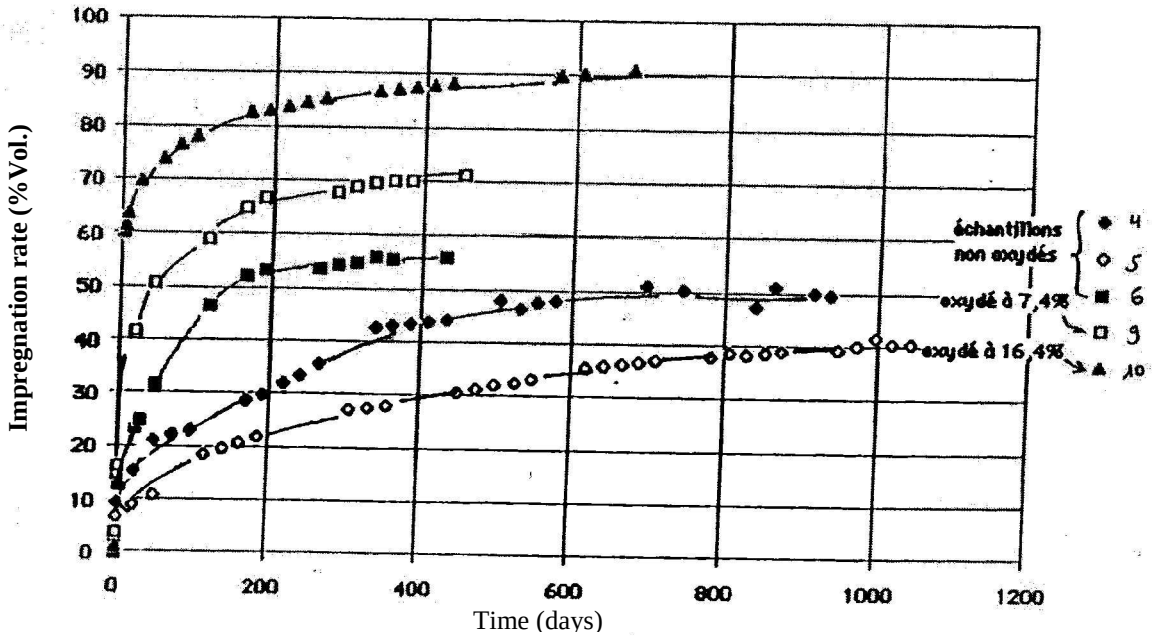


FIGURE 5: EFFECT OF RADIOLYTIC CORROSION ON THE SATURATION RATE

1.3. Tests on Magnox-type graphite

The results of these studies are summarised in the document called "Assessment of management modes for graphite from reactor decommissioning"[7] and mainly aim at identifying how graphite should be managed after reactor operation (particularly for Magnox reactors).

Tests were performed on graphite blocks to study water penetration in the case of deep-sea waste disposal. The authors remarked that non-irradiated graphite blocks weighing several kilos (14 and 18 litres) after immersion in water under pressures of 450 bar and 928 bar were not visibly damaged and gained between 7.6% and 9.4% mass in water. The data cannot be used to calculate a saturation rate. The tests performed on irradiated samples (h=48 mm Φ=48 mm) show the following mass gain (Table 5).

Test conditions	Immersion time (days)	Mean weight gain (%)
Simulated groundwater (1 bar, 25°C)	150	12.4
Demineralised water (1 bar, 20°C)	150	12.5
Simulated seawater (450 bar, 2.5°C)	106	15.2
Simulated seawater (1 bar, 20°C)	137	9.1

TABLE 5: MASS GAIN OF IRRADIATED GRAPHITE BLOCKS DURING LEACHING

It can be seen that the irradiated samples were impregnated with more water, i.e. 9.1% to 12.4% under 1 bar and 15.2% under 450 bar, which is twice that of the non-irradiated samples.

1.4. Tests on Hanford graphite samples (USA)

During leaching tests on samples performed by the CEA and the US DOE, water impregnation in irradiated graphites from Hanford was measured at the end of the tests [8]. The results are shown in Table 6 and show that the mass gain of these samples is about 14% in 91 days, which corresponds to a saturation rate of 75% in relation to the total porosity.

Sample	Initial mass	Dimensions	volume (cm^3) / surface (cm^2)	Apparent density	Total porosity	Final mass	Mass difference		Saturation rate Total %
	g	(mm)		(g/cm^3)	ref (2.266)	g (+91d)	g	%	%
D1	631.39	Φ=79.4 H=79.1	v=391.6 s=296.3	1.612	28.9%	715.52	84.1	13.3%	74.4%
E2	636.24	Φ=79.6 H=79.4	v=395.1 s=298.1	1.61	28.9%	727.13	90.9	14.29%	79.48%
G3	642.62	Φ=79.5 H=79.2	v=393.14 s=297.1	1.635	27.8%	724.86	82.2	12.80%	75.07%

TABLE 6: WATER IMPREGNATION IN HANFORD GRAPHITES DURING LEACHING TESTS

1.5. Summary of data

The preliminary data collected on nuclear-grade fuel sleeve and stack graphites, as well as on non irradiated and irradiated samples, shows that:

- Water impregnation in the porous medium of non irradiated graphite is relatively slow and remains incomplete for durations up to 90 days. The saturation rate follows a proportional V/S law and seems to be related to a diffusion process (linearity according to a square-root-of-time scale),

- Tests performed at high pressure show that non irradiated graphite absorbs about 15 wt% of water, which can be considered as the maximum mass gain,

- Irradiation increases the kinetics and the impregnation rate.

There is nevertheless very little information available which is why it needs to be extended to cover G2 and St Laurent A2 samples

EXPERIMENTAL MEASUREMENTS

The study involved monitoring the change in the mass of samples immersed in water as over time. Two techniques were used: continuous measurements for immersed samples suspended from a precision electronic balance, and intermittent measurements of the mass variations in immersed samples placed in experimental vessels.
In the first case, the sample was hung from a Sartorius balance beam and fully immersed in a container filled with ultrapure water. This configuration made it possible to continuously measure any changes in the apparent mass of the samples in water. As the water impregnates the sample, the buoyant force decreases and the apparent mass increases, which therefore makes it possible to determine the water mass having impregnated the sample. Measurements were taken over periods of about 10 to 40 days depending on the sample.
In order to determine the long-term impregnation kinetics, the samples were placed in reaction vessels filled with ultrapure water while making sure the S/V remained the same. The sample masses were measured regularly as follows: The sample was removed from the reaction vessel, gently wiped with paper towelling to remove the surface layer of water, weighed, and then put back in the reaction vessel. The sample-wiping operation - the most delicate - was performed by the same person to ensure the reproducibility of all the weighing operations.

G2 REACTOR

1.6. Sample preparation

1.6.1. G2 non-irradiated samples

The reference brick for the non-irradiated samples was taken from a stock of bricks located under the G2 reactor. The 200 mm side cross-section of the brick showed two half-channels with a diameter of 70 mm. This is the geometry of G2 moderator bricks which are made from a special coke mixture. A succession of 3 mm lamellae were cut from this brick using a LECD wire saw and transferred to the different laboratories taking part in the programme. The initial lamella sent to the LARC laboratory was cut into smaller samples with a wire saw to be used in the different tests (see plan). The samples were characterised by means of geometric density measurements, He pycnometry, Hg porosimetry, X-ray diffraction and Raman spectroscopy. The results and the measurement protocols are published in the report "Characterisation of G2 stack graphite before and after irradiation"[2].
The following table lists all the physical characteristics of the samples. The closed porosity of the samples is about 4%.

Test	Reference under sample	Mass (g)	Dimensions (cm^3)	Surface (cm^2)	Volume (cm^3)	S/V (cm^{-1})	ρ_G	Total porosity (%)	Monitoring
B1	5-2	3.6199	1.5*1.4*1	10.5±0.6	2.25±0.06	4.66±0.14	1.61±0.04	29.0±0.8	continuous
B2	5-1	7.2085	1.5*1.5*2.0	16.3±1.0	4.41±0.13	3.69±0.13	1.63±0.05	27.9±0.8	continuous
B3	5-11	10.7028	1.5*1.4*2.9	21.5±1.7	6.39±0.25	3.37±0.14	1.68±0.06	25.9±1.0	continuous
D1	5-3	10.477	1.5*1.4*2.9	21.5±1.4	6.33±0.21	3.39±0.13	1.66±0.06	27.0±0.9	intermittent
D2	5-8	10.9432	1.5*1.5*2.9	22.0±0.9	6.59±0.13	3.34±0.07	1.66±0.03	26.7±0.5	intermittent
D3	5-9	11.9068	3*2.9*0.85	27.2±1.7	7.30±0.22	3.73±0.13	1.63±0.05	28.0±0.9	intermittent

TABLE 7: CHARACTERISTICS OF NON IRRADIATED G2 SAMPLES FOLLOWIN WATER IMPREGNATION

The results were determined with an expanded uncertainty k=2

Test	Sample Reference	Mass (g)	Dimensions (cm^3)	Surface (cm^2)	Volume (cm^3)	S/V (cm^{-1})	ρ_G	Total porosity (%)	Monitoring
EtOH-1	5-10	15.526	3.01*1.07*2.88	29.8±1.5	9.2±0.2	3.24±0.09	1.68±0.04	25.7±0.7	intermittent

TABLE 8: CHARACTERISTICS OF NON IRRADIATED G2 SAMPLE AFTER IMPREGNATION IN A MIXTURE OF WATER AND ETHANOL (10 WT%)

The results were determined with an expanded uncertainty k=2

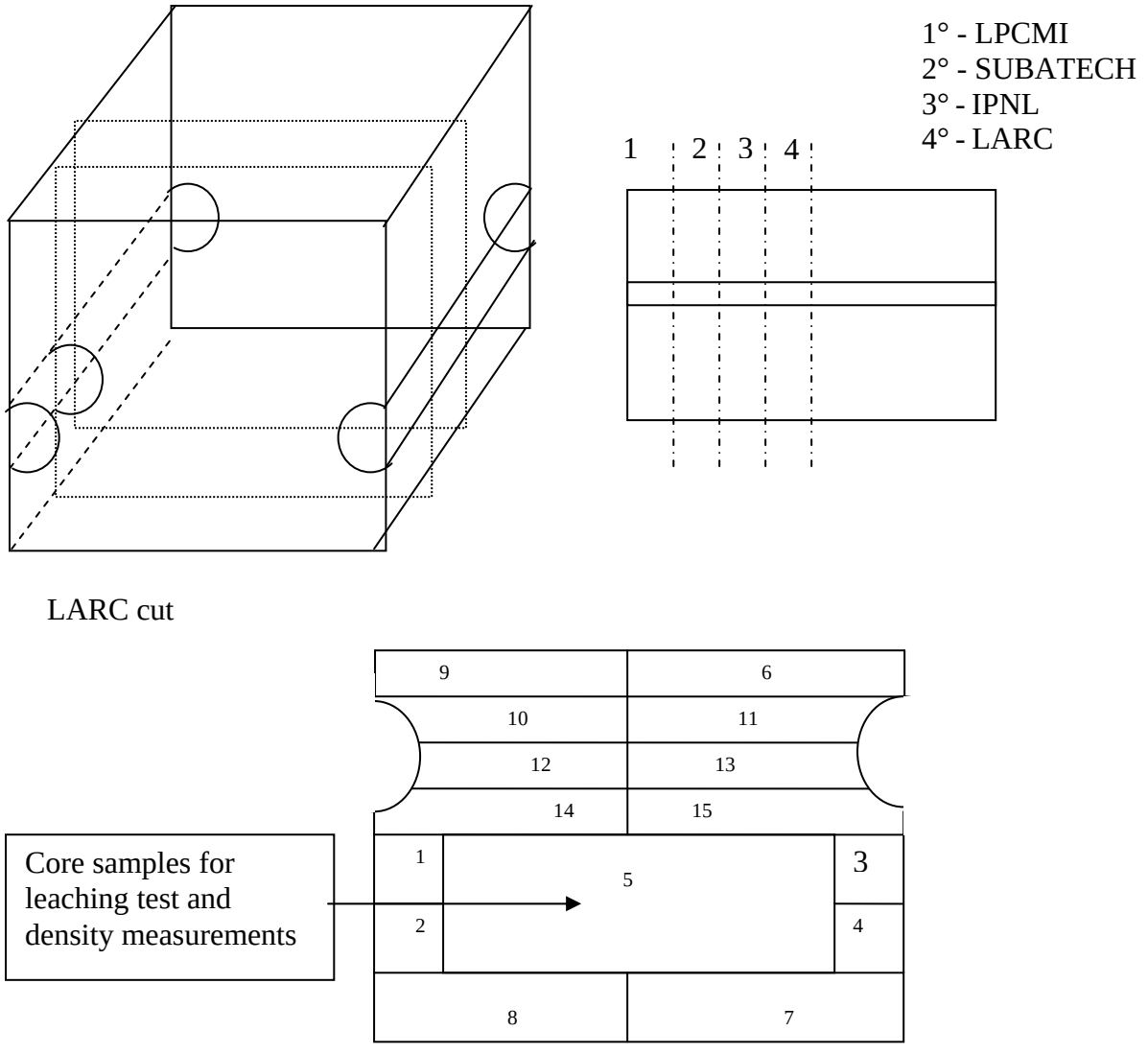


FIGURE 6: CROSS-SECTIONS OF THE NON-IRRADIATED G2 GRAPHITE BRICK

1.6.2. G2 irradiated samples

We chose four core samples from different places in the lower half of the reactor: three in the moderator (Nos 27, 32 and 42) and one in the reflector (No. 46). It was therefore possible to include the leaching results of core sample No. 36 – located between core sample Nos 32 and 42 – from a previous study [9] with the results obtained for our core samples. The five core samples were more or less equidistant from each other, as shown in Figure 7.

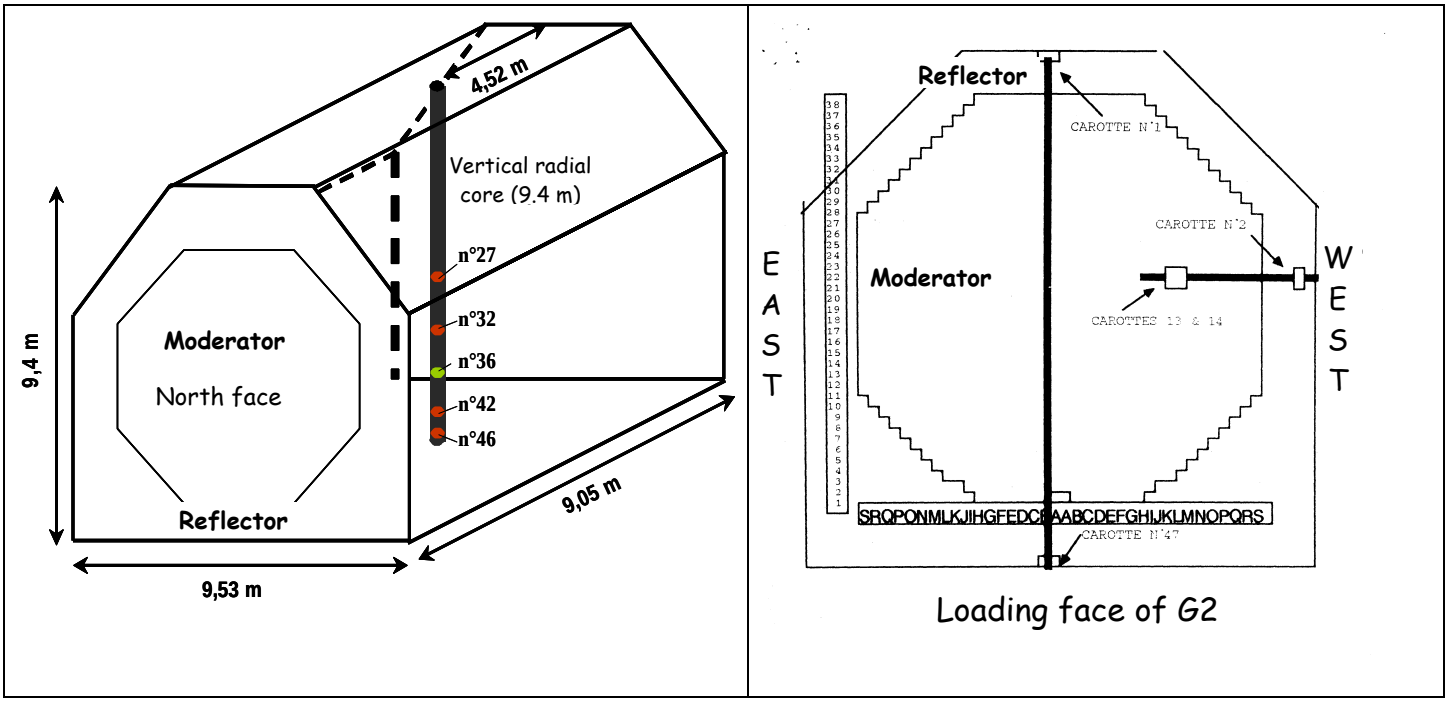


FIGURE 7: REPRESENTATION OF G2 REACTOR WITH VERTICAL CORING AND LOCATION OF CORE SAMPLES

Table 9 shows the sampling heights and the reactor operating temperature relative to the samples chosen for the impregnation and leaching tests.

Sample No.	Position	Presumed initial coke	Sampling height (m)	Temperature (°C)[10]
G2-27	Moderator	Special A coke	13.60-13.80	327
G2-32	Moderator	Special A coke	14.60-14.80	320
G2-42	Moderator	Special A coke	16.60-16.80	309
G2-46	Reflector	Lockport coke	17.40-17.60	<250

TABLE 9: G2 SAMPLES CHOSEN FOR LEACHING TESTS

Sub-samples were produced to conduct these tests, in particular two sub-samples located near the centre of the core samples: a cylindrical sample and a cubic-shaped sample. The tables below show the characteristics of the samples used such as their dimensions, geometric density, surface area and volume.

	Mass	Average dimensions	Density ρ_G	Total porosity Calculated open[#1] Calculated closed[#2]	Surface	Volume	S/V sample	S/V leachate
Reference	(g)	(cm^3)		%	cm^2	cm^3	cm^{-1}	cm^{-1}
G2-27-7A	12.1629	1.53*1.53*3.02	**1.72±0.03**	24.1±**0.3%** **22.1±1.8%** 2.0±**1.5**%	**23.2±1.4**	**7.1±0.1**	3.3±**0.2**	**0.154±0.002**
G2-32-6A	10.5228	1.47*1.46*3.12	**1.58±0.04**	30.0±0.4% 27.0±**0.9**% 3.1±**0.5**%	**22.5±1.4**	**6.7±0.1**	3.4±**0.2**	**0.151±0.002**
G2-42-6A	13.2756	1.61*1.52*3.12	**1.74±0.06**	23.3±**0.4%** 19.3±**1.7**% 4.0±**1.3**%	**25.0±1.5**	**7.6±0.1**	3.3±**0.2**	**0.150±0.002**
G2-46-5A	11.9283	1.6*1.48*3.02	**1.67±0.03**	26.4±**0.4%** 21.4±**1.0**% 5.0±**0.6**%	**24.1±1.4**	**7.1±0.1**	3.4±**0.2**	**0.167±0.002**

TABLE 10: CHARACTERISTICS OF SAMPLES – G2 CUBE

	Mass	Average dimensions	Density ρ_G	Total porosity Calculated open[#1] Calculated closed[#2]	Surface	Volume	S/V sample	S/V leachate
Reference	(g)	Diam.*L. (cm*cm)		%	cm^2	cm^3	cm^{-1}	cm^{-1}
G2-27-6	80.0304	6.32*1.53	**1.67**±0.02	**26.4**±0.4% **24.4±1.9%** 2.0±**1.5**%	**93.1±1.3**	**48.0±0.7**	1.94±**0.04**	0.62±**0.01**
G2-32-5	72.0947	6.32*1.40	**1.64**±0.02	**27.6**±0.4% **24.6±0.9%** 3.1±**0.5**%	**90.5±1.4**	**43.9±0.7**	2.06±**0.04**	0.60±**0.01**
G2-42-5	82.044	6.32*1.50	**1.74**±0.02	**23.1**±0.4% **19.1±1.7%** 4.0±**1.3**%	**92.5±1.3**	**47.1±0.7**	1.97±**0.04**	0.62±**0.01**
G2-46-4	80.8629	6.32*1.56	**1.65**±0.02	**27.1**±0.4 **22.1±1.0%** 5.0±**0.6**%	**93.7±1.3**	**48.9±0.7**	1.91±**0.04**	0.62±**0.01**

TABLE 11: CHARACTERISTICS OF SAMPLES – G2 CYLINDER

#1 Open porosity calculated as the difference between the total porosity inferred from the geometric measurements and the mean of the closed porosities

#2 Mean closed porosity of the samples measured in report ref. DEC/SA3C/LARC 09/008

1.7. Measurements on non irradiated graphite samples

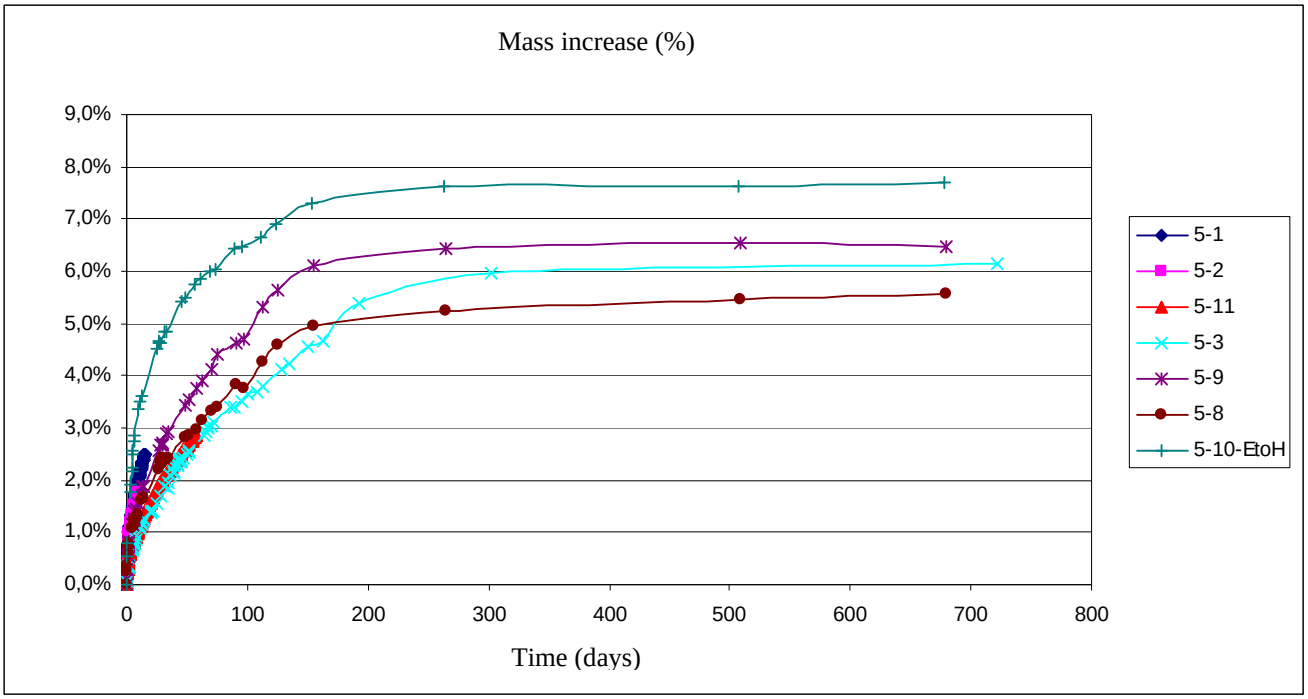
Figure 8 shows the change in the sample masses and the saturation rate expressed in relation to open porosity.

Comparison between tests shows good reproducibility between the different measurements taken both continuously over short periods and intermittently over longer periods.
It can be seen that water impregnation in non-irradiated graphite samples is relatively slow. Impregnation continues over rather long periods (250 days) during which the process is much slower. Saturation rates reach a maximum of about 40% to 45% open porosity in the samples. These rates are much higher than those measured by Costes *et al.*[5,6], which shows that their measurements were not performed over long enough periods (25 days) despite the apparent stabilisation of the sample masses. Nevertheless, the saturation rates obtained for the same period of time are comparable (10% to 17% in 15 days) between the two test series.

Adding ethanol (10 wt%) improves impregnation: the kinetics and saturation rate increase significantly. Adding ethanol to water helps to lower the surface tension of the mixture and therefore encourage its impregnation in a hydrophobic solid.

Solution	Surface tension (mN/m)
Water	72.8
Ethanol	22
Water+10%m Ethanol	52

TABLE 12: SURFACE TENSION AT 20℃



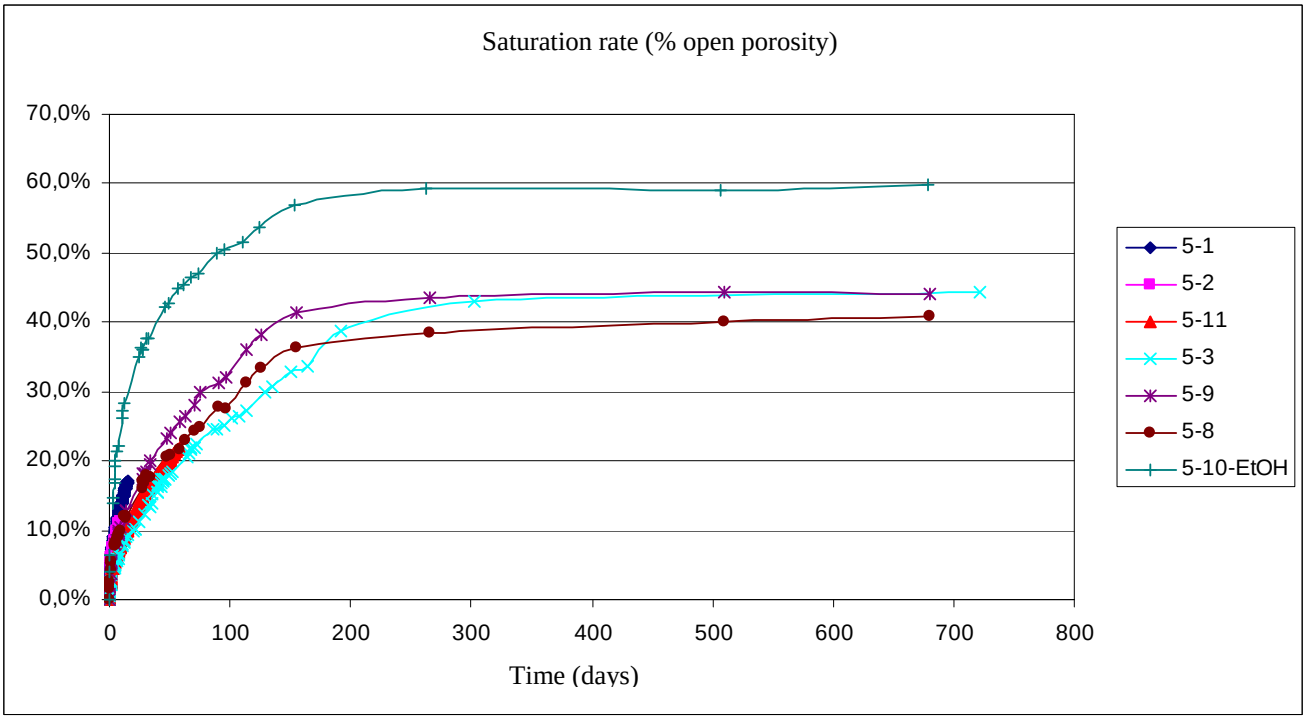
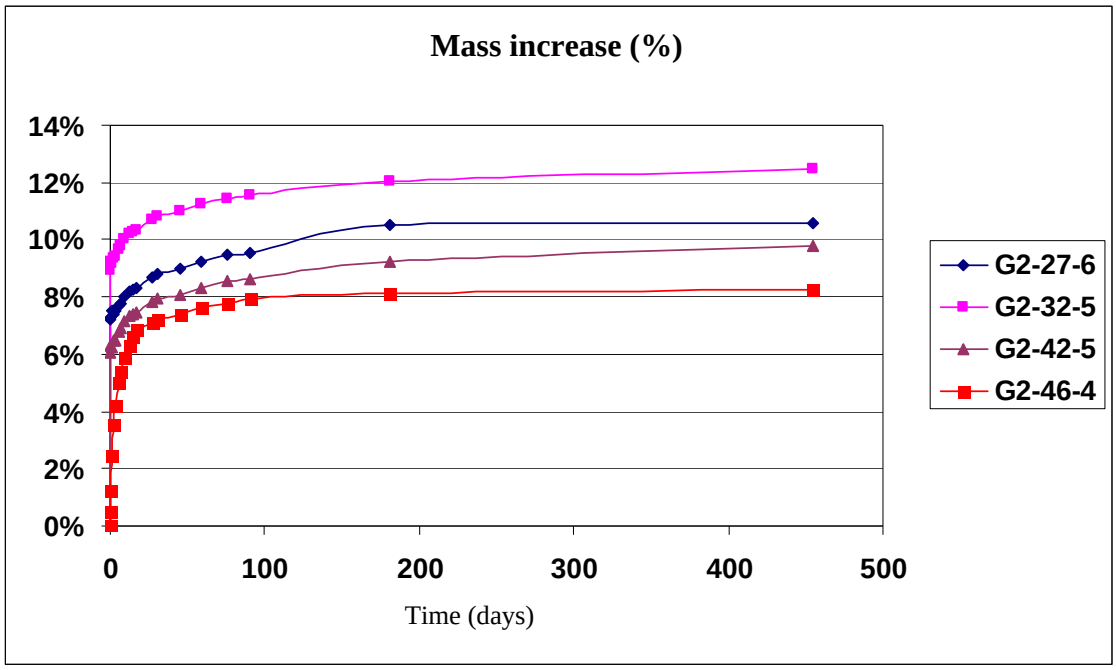


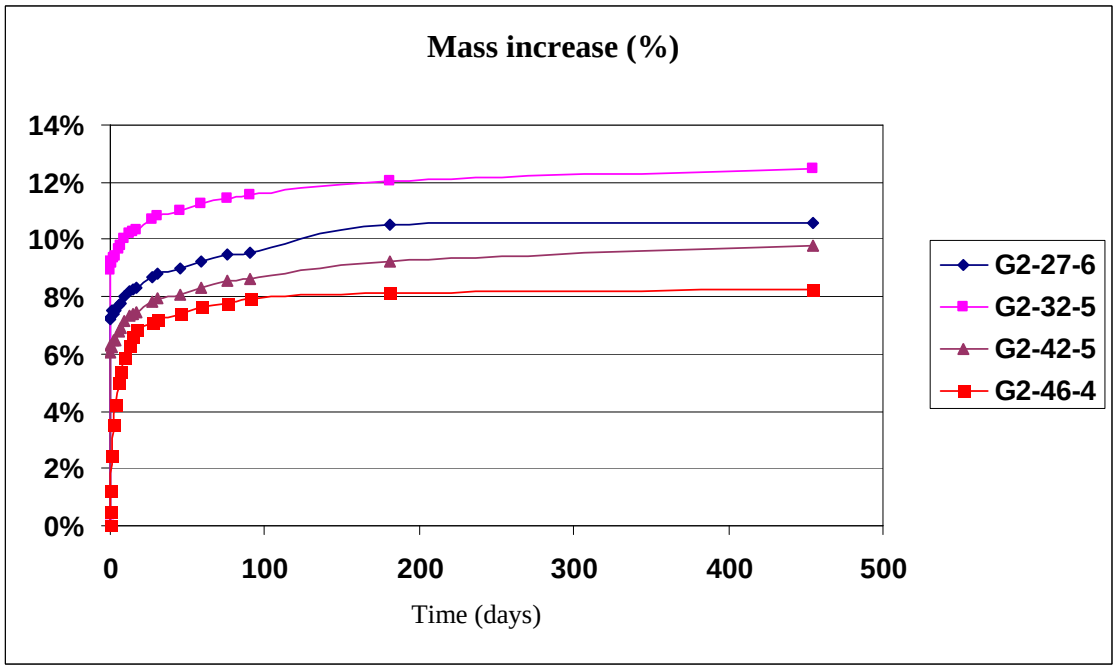
FIGURE 8: CHANGE IN NON IRRADIATED G2 SAMPLE MASSES AND THE SATURATION RATE

1.8. Measurements on irradiated samples

Figures 9 and 10 show the change in the sample masses and the saturation rate expressed in relation to the open porosity.

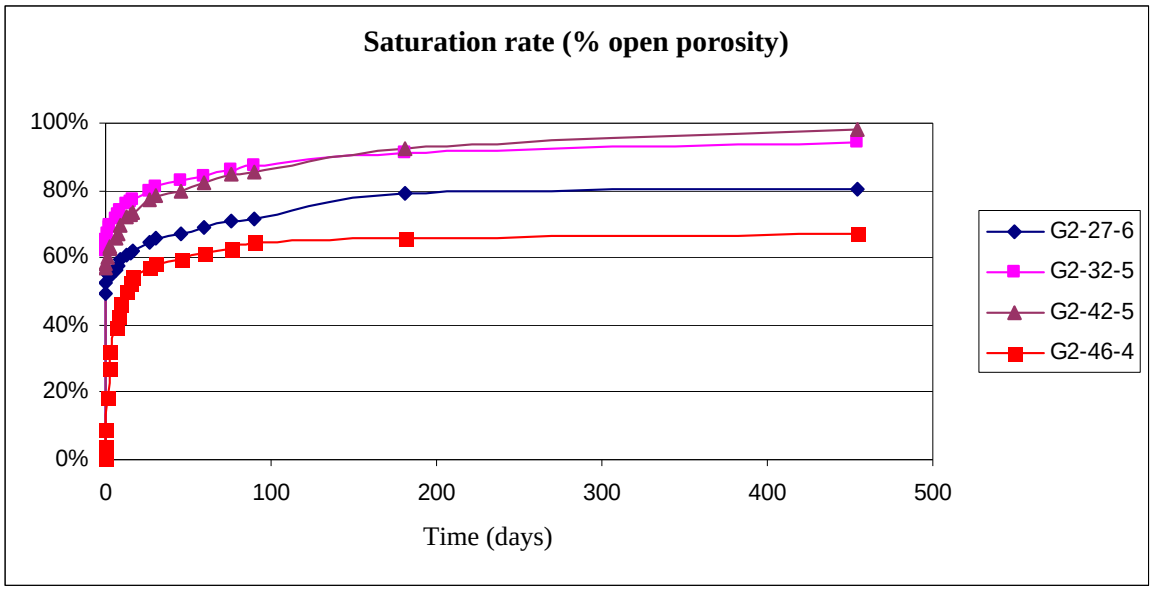


(A)

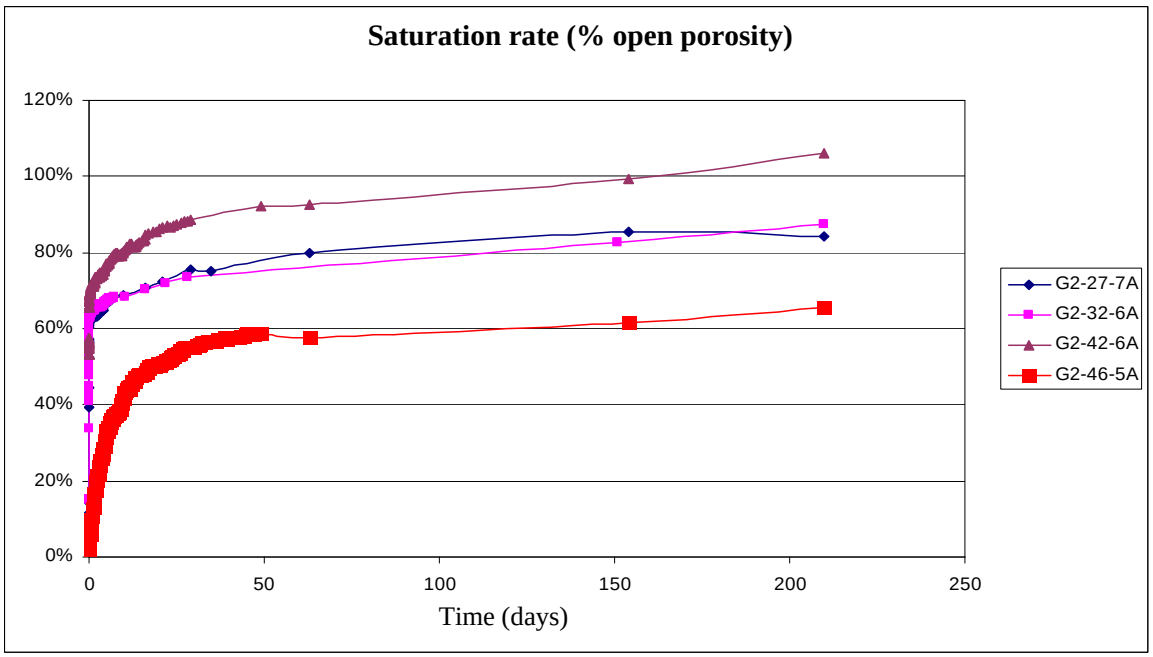


(B)

FIGURE 9: CHANGE IN THE MASS OF IRRADIATED G2 SAMPLES (CYLINDER (A) AND CUBE (B))



(A)



(B)

FIGURE 10: SATURATION RATE OF IRRADIATED G2 SAMPLES (CYLINDER (A) AND CUBE (B))

Considering the uncertainty on the measurement of sample volumes, open porosities and mass gains, the following relative uncertainty was associated with each test:

G2-27- 6: 8%	G2-32-5: 4%	G2-42-5: 9%	G2-46-4: 5%
G2-27- 7A: 9%	G2-32-6A: 4%	G2-42-6A: 9%	G2-46-5A: 5%

		G2-27	G2-32	G2-42	G2-46
Mass gain	Cylinder	11%	12%	9%	8%
	Cube	11%	15%	12%	8%
	Mean	**11%**	**13%**	**11%**	**8%**
	Deviation	**0.2%**	**2.0%**	**1.8%**	**0,2%**
Saturation rate/ total porosity	Cylinder	73±1%	81±2%	76±2%	54±1%
	Cube	76±2%	79±2%	86±2%	53±1%
	Mean	**75%**	**80%**	**81%**	**54%**
	Deviation	**1.6%**	**1.1%**	**6.8%**	**0.4%**
Saturation rate/ open porosity	Cylinder	79±6%	91±4%	92±8%	66±3%
	Cube	84±7%	87±3%	106±9%	65±3%
	Mean	**81%**	**90%**	**98%**	**66%**
	Deviation	**2.1%**	**1.9%**	**8.1%**	**0.2%**

TABLE 13: WATER IMPREGNATION IN IRRADIATED G2 SAMPLES (MASS GAIN AND MAXIMUM SATURATION RATE)

The two tests performed on samples with different geometries produce identical results.

For the moderator samples:

- The water impregnation kinetics in the samples are fast,
- The mass gain is about 12% on average,
- The water saturation rates are high, reaching almost 80% in relation to the total porosity and an average of 90% in relation to the open porosity. Water seems to quickly occupy all accessible porosity. Measurements taken by Hg porosity on samples from the same cores had shown that these samples were mainly macroporous (about 80% of the porosity with an apparent pore diameter ranging between 1 and 30 µm) [2].

For the reflector samples:

- The water saturation rate is slightly slower than that of the moderator samples,
- The mass gain is lower at about 8% (compared with 12% for moderator samples),
- The saturation rate reaches a plateau at around 54% of the total porosity, i.e. 66% of the open porosity. Water thus penetrates at a slower rate and does not occupy all of the total accessible porosity.

These differences can be explained by the lower irradiation at a lower temperature and without the coolant gas of the reflector sample, as well as by the type of the reflector graphite which is made from Lockport L coke as opposed to the moderator graphite which is made from Special A coke.

1.9. Comparison of tests on G2 non irradiated and irradiated graphite samples

Comparison of the saturation rate between non irradiated and irradiated samples is shown in Figure 11 below for samples made from special A coke (moderator graphite and non irradiated graphite).

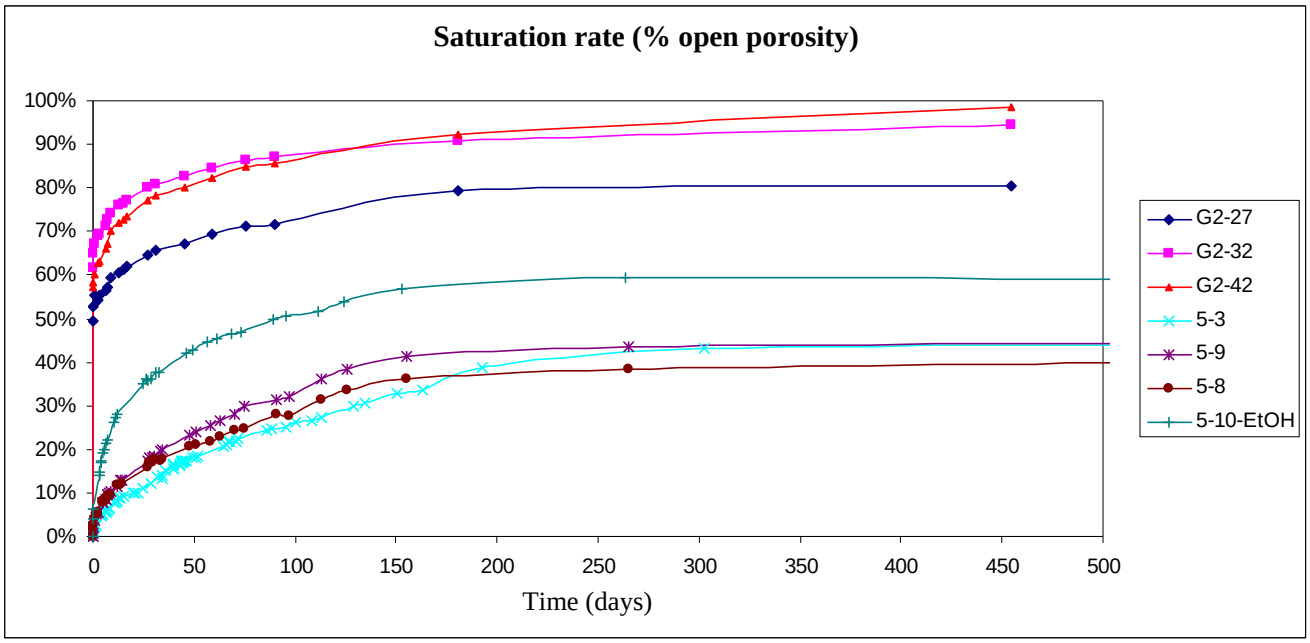


FIGURE 11: COMPARISON OF SATURATION RATES FOR G2 NON IRRADIATED AND IRRADIATED GRAPHITE SAMPLES MADE FROM SPECIAL A COKE (MODERATOR)

It can be clearly seen that water impregnation is greater in irradiated samples which occurs with faster kinetics than those for non-irradiated samples. It can also be seen that the saturation rate for the water + ethanol mixture is between the saturation rates for irradiated and non-irradiated graphite tests.

The results show that the water impregnation process is significantly modified when the graphite has been in reactor conditions. It results in a much faster impregnation with practically all of the accessible porosity (90%) in the irradiated graphite being filled contrary to non-irradiated samples.

SLA2 REACTOR

1.10. Sample preparation

1.10.1. SLA2 non-irradiated samples

These cylindrical samples were about 8 cm long with a diameter of about 1.2 cm. They were made from LIMA coke as is the case for Bugey reactor graphite. Several sub-samples were cut from the cylinders to obtain shorter samples. The density of all available samples was measured and revealed a mean of 1.70±0.03 g/cm^3, with densities ranging between 1.647 and 1.734. The total porosity was calculated at about 25%. Helium pycnometry measurements were performed on non irradiated SLA2 graphite samples. These measurements show a total porosity of 24.7% with an open porosity of 18.9% and a closed porosity of 5.8%. This closed porosity is assumed to remain constant throughout our interpretations when it comes to calculating the saturation rates for all non-irradiated samples.

The sample characteristics are given in Table 14.

Test	Sample references OP3784-	Mass (g)	Dimensions Diam.*L (cm*cm)	Surface (cm^2)	Volume (cm^3)	S/V (cm^{-1})	ρ_G	Total porosity (%)	Monitoring
Z1	CD38870 Z	4.0085	1.20*2.08	10.1±0.3	2.35±0.03	4.3	1.70±0.02	24.8%	Intermittent
Z2	CD38866 Z	7.7454	1.20*4.09	17.7±0.4	4.63±0.02	3.8	1.67±0.01	26.1%	Intermittent
XY 1	CD38866 XY	7.5475	1.20*3.93	17.1±0.4	4.44±0.02	3.8	1.70±0.01	25.1%	Intermittent

TABLE 14: CHARACTERISTICS OF NON-IRRADIATED SLA2 SAMPLES

1.10.2. SLA2 irradiated samples

The SLA2 graphite samples available in the UNGG sample library at the LARC laboratory chosen for the leaching tests were taken from two channels: F10M16-C20 and F7M15-C19 located at a radius of 5 m and 2.95 m respectively from the reactor centre with variable sampling heights. Three samples per channel were chosen for the structural characterisation studies and the leaching tests.

Channel	Well/Tube	Height	Sample No.	Temperature (°C)	Thermal neutron flux ($n.cm^{-2}.s^{-1}$)
F10M16	C20	2070	SLA2-44	435	$6.8.10^{12}$
F10M16	C20	7280	SLA2-55	310	$7.1.10^{12}$
F10M16	C20	8660	SLA2-58	270	$3.4.10^{12}$
F7M15	C19	2070	SLA2-124	455	$5.7.10^{12}$
F7M15	C19	7280	SLA2-135	310	$5.8.10^{12}$
F7M15	C19	8660	SLA2-138	270	$2.7.10^{12}$

TABLE 15: SLA2 GRAPHITE SAMPLES CHOSEN FOR THE LEACHING TESTS

The samples were initially provided in the shape of cylindrical cores whose approximate dimensions were: 19 mm diameter and 50 mm high. Some measurements required cutting up some samples into semi-circles about 10 mm thick. For the six samples chosen for the leaching tests, these semi-circles were used to determine the initial chlorine-36 activity and to measure porosity (helium pycnometry and mercury porosimetry). The rest of the core, i.e. about 40 mm long, was reserved for continuous water impregnation tests. Figure 12 shows how the samples were divided up for the different analyses.

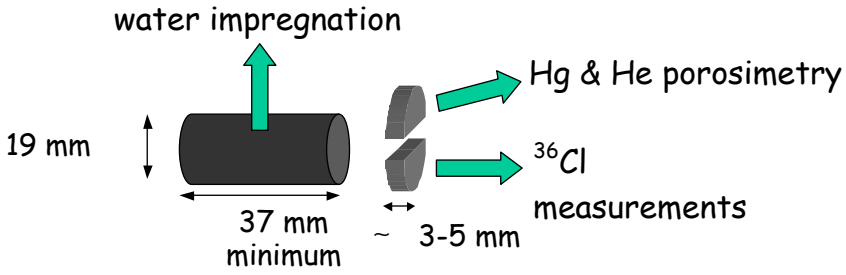


FIGURE 12: SLA2 GRAPHITE CORE AND ITS DISTRIBUTION FOR THE DIFFERENT ANALYSES

	Mass	Average dimensions	Density ρ_G	Total porosity	Surface	Volume	S/V sample	S/V leachate
Reference	(g)	Diam.*L. (mm*mm)		%	cm^2	cm^3	cm^{-1}	cm^{-1}
SLA2-44	21.9988	19*48	1.61±0.05	29.1±0.9	**34**±1	**13.6**±0.4	2.5±0.1	0.229±0.004
SLA2-55	17.9422	19*39	1.62±0.04	28.6±0.8	**29**±1	**11.1**±0.3	2.6±0.1	0.193±0.006
SLA2-58	22.1746	19*47	1.68±0.04	26.0±0.7	**33.5**±0.9	**13.2**±0.3	2.5±0.1	0.223±0.007
SLA2-124	22.0483	19*50	1.55±0.05	31.5±1.1	**35.7**±1.1	**14.2**±0.4	2.5±0.1	0.238±0.008
SLA2-135	23.1589	19*51	1.60±0.09	29.2±1.7	**36.1**±1.9	**14.5**±0.8	2.5±0.2	0.241±0.013
SLA2-138	22.0355	19*50	1.56±0.12	31.0±2.4	**35.4**±2.7	**14.1**±1.1	2.50±0.3	0.236±0.018

TABLE 16: CHARACTERISTICS OF SLA2 IRRADIATED SAMPLES

As the open porosity could not be determined directly from the samples used in the impregnation tests but only from low-mass pieces taken from the channel-side of the core ends, we chose to use the data collected from previous studies [11, 12].

The samples from these studies were geometrically similar to the samples used to take several different measurements. The following tables show that the closed porosity varies between 3% and 5%; we took into account a closed porosity of 4% for all irradiated samples.

Sampling height (mm)	Geometric density (g/cm^3)	Wear Ref d=1.684 g/cm^3	Total porosity Ref d=2.266 g/cm^3	Open porosity (bromobenzene)	Closed porosity
9260	1.666	1.05%	26.46%	21.69%	4.77%
8660	1.634	2.98%	27.90%	23.97%	3.93%
8270	1.615	4.11%	28.74%	24.33%	4.41%
6890	1.578	6.32%	30.38%	26.76%	3.62%
5120	1.559	7.45%	31.22%	26.42%	4.81%
4480	1.553	4.79%	31.48%	28.08%	3.40%
3450	1.600	5.00%	29.40%	25.83%	3.57%
2460	1.630	3.24%	28.09%	24.49%	3.60%
1680	1.590	5.56%	29.81%	24.48%	5.33%
300	1.733	-2.89%	23.53%	18.19%	5.34%

TABLE 17: POROSITY AND DENSITY OF SAMPLES FROM CHANNEL F10M10-C20 [11]

Sampling height	Geometric density	Wear Ref d=1.684 g/cm^3	He pycnometry density (+/-0.25%)	Total porosity Ref d=2.266g/cm^3	Open porosity %		Closed porosity
(mm)	(g/cm^3)		(g/cm^3)	(%)	(He)	(Hg)	(%)
9260	1.65	2.0%	2.12	25.9%	22.4%	22.3%	3.7%
8660	1.64	2.6%	2.15	26.3%	23.7%	23.5%	2.6%
3060	1.60	5.0%	2.14	28.1%	25.3%	n.m	2.9%
2460	1.62	3.8%	2.12	27.2%	23.7%	24.4%	3.7%
2070	1.61	4.4%	2.10	27.7%	23.5%	21.8%	4.4%
1680	1.59	5.6%	2.11	28.6%	24.8%	22.9%	3.9%
300	1.68	0.2%	2.13	24.5%	21.1%	22.4%	3.4%

TABLE 18: EXTRACT OF DATA FOR SAMPLES FROM CHANNEL F5M19-C20 [12]

1.11. Measurements on non irradiated graphite samples

Figure 13 shows the change in the sample masses and the saturation rate expressed in relation to the open porosity.

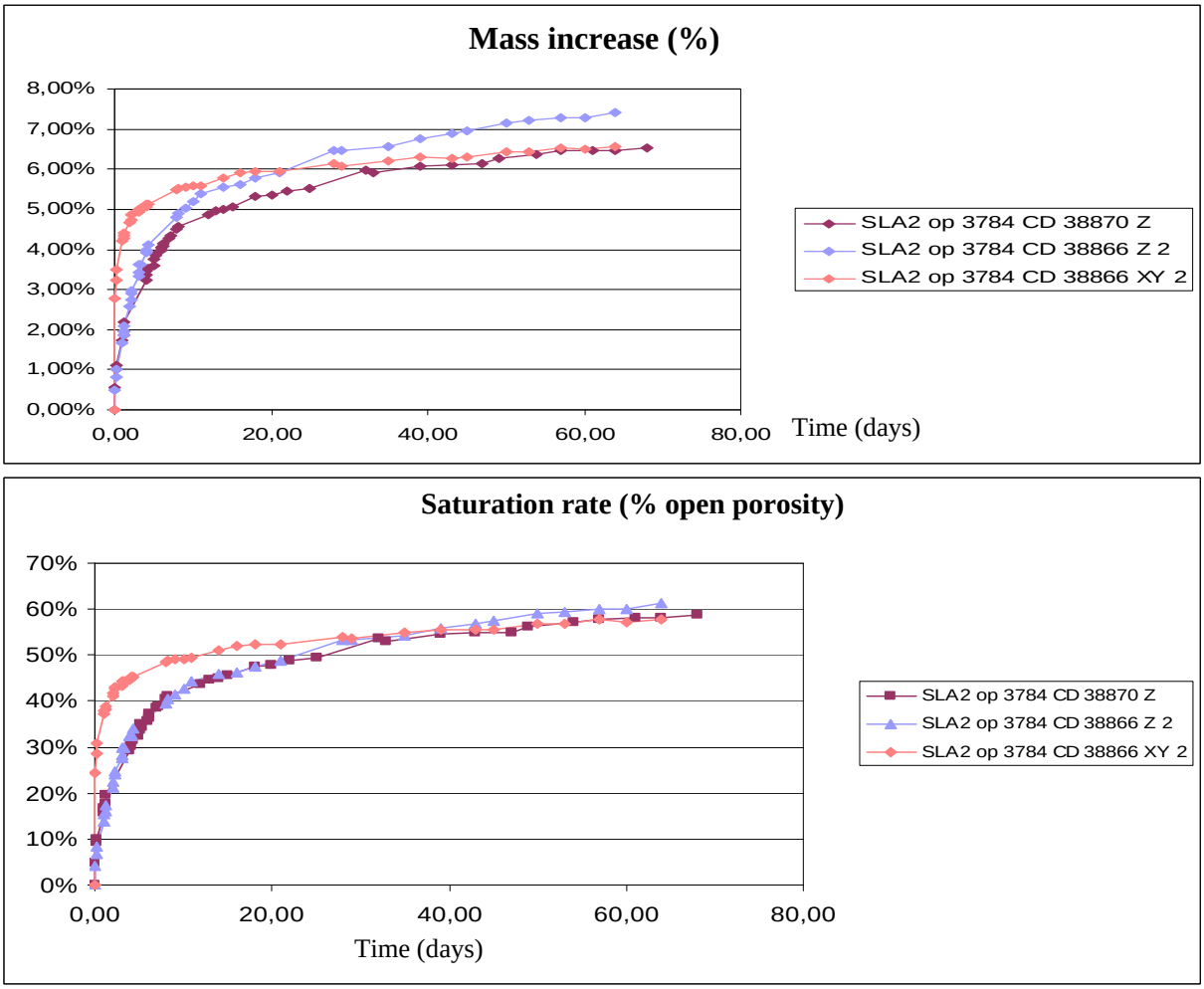


FIGURE 13: CHANGE IN NON IRRADIATED ST LAURENT A2 SAMPLE MASSES AND THE SATURATION RATE

Considering the uncertainty on the measurement of sample volumes, open porosities and mass gains, a relative uncertainty of 4% was associated with each test.

These tests show a slight difference in behaviour between the sample taken in the XY plane and those taken along the extrusion axis (Z) on the initial mass gain kinetics. The core sample taken from the XY plane undergoes impregnation much faster than the two samples cored along the Z axis. Following this initial period of impregnation however, the behaviour is identical and the saturation rates are similar after 40 days, reaching about 55% of the open porosity.

It can also be seen that despite the apparent stabilised mass gains, impregnation continues but with slower kinetics.

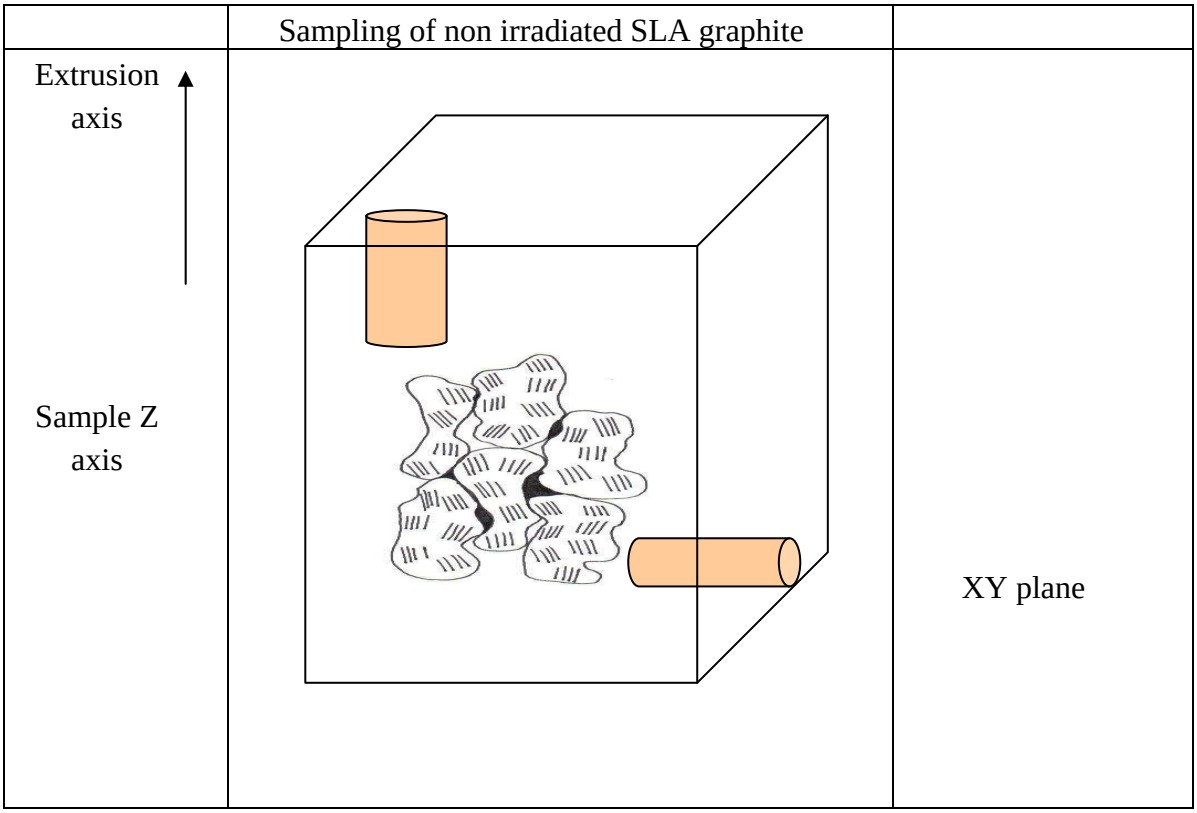


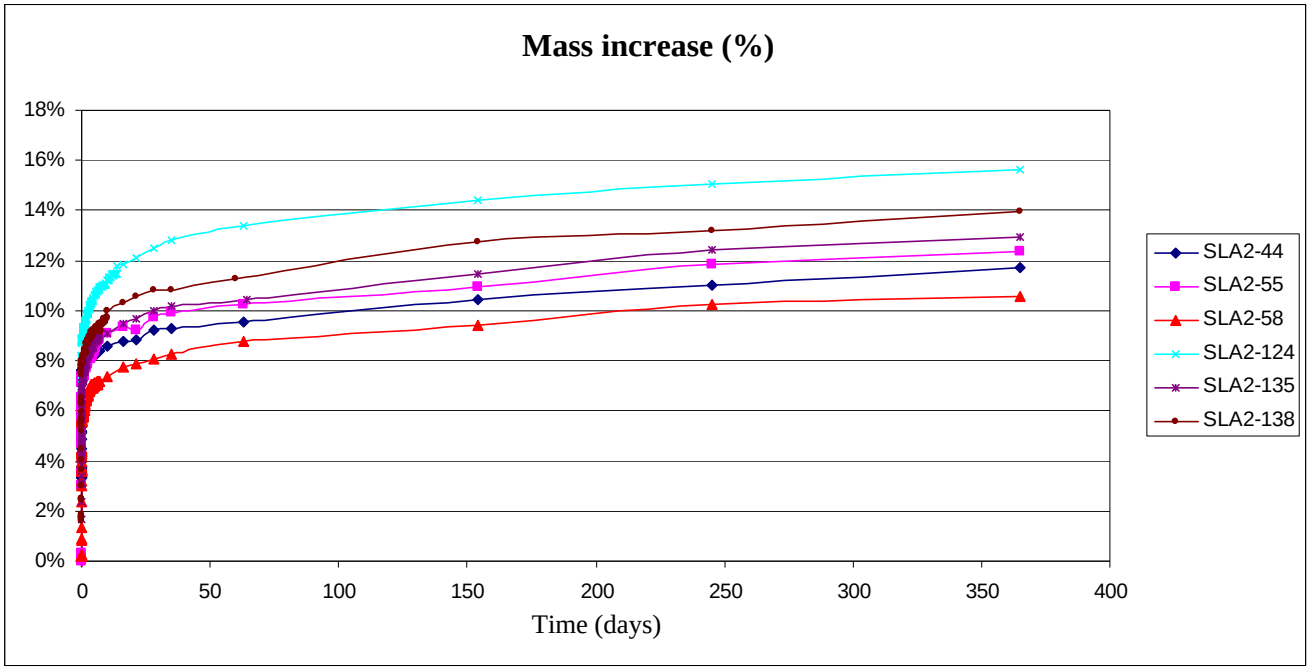
FIGURE 14: LOCATION OF SAMPLES TAKEN FROM THE ST LAURENT A2 REACTOR IN RELATION TO THE SAMPLING PLANE

1.12. Measurements on irradiated graphite samples

Figure15 and Table 19 show the change in the immersed sample masses and the saturation rate. As for the G2 samples, it can be seen that the impregnation kinetics are fast. Depending on the samples, the saturation rate varies between 65% and 77% in relation to the total porosity and between 75% and 88% in relation to the open porosity, which indicates high water impregnation in the graphite porosity after 365 days.

	SLA2-44	SLA2-55	SLA2-58	SLA2-124	SLA2-135	SLA2-138
Channel	F10M16	F10M16	F10M16	F7M15	F7M15	F7M15
Well	C20	C20	C20	C19	C19	C19
Height (mm)	2070	7280	8660	2070	7280	8660
Thermal neutron flux ($n.cm^{-2}.s^{-1}$)	$6.8.10^{12}$	$7.1.10^{12}$	$3.4.10^{12}$	$5.7.10^{12}$	$5.8.10^{12}$	$2.7.10^{12}$
Temperature (°C)	435	310	270	455	310	270
ρ_G	1.61±0.05	1.62±0.04	1.68±0.04	1.55±0.05	1.60±0.09	1.56±0.12
Mass gain (%)	11.7±0.1	12.4±0.1	10.6±0.1	15.6±0.1	12.9±0.1	13.9±0.1
Saturation rate Total porosity (%)	65±3	70±3	68±3	77±4	71±6	70±37
Saturation rate Open porosity (%)	75±6	81±6	81±6	88±7	82±10	81±11

TABLE 19: WATER IMPREGNATION IN IRRADIATED SLA2 SAMPLES (MASS GAIN AND MAXIMUM SATURATION RATE)



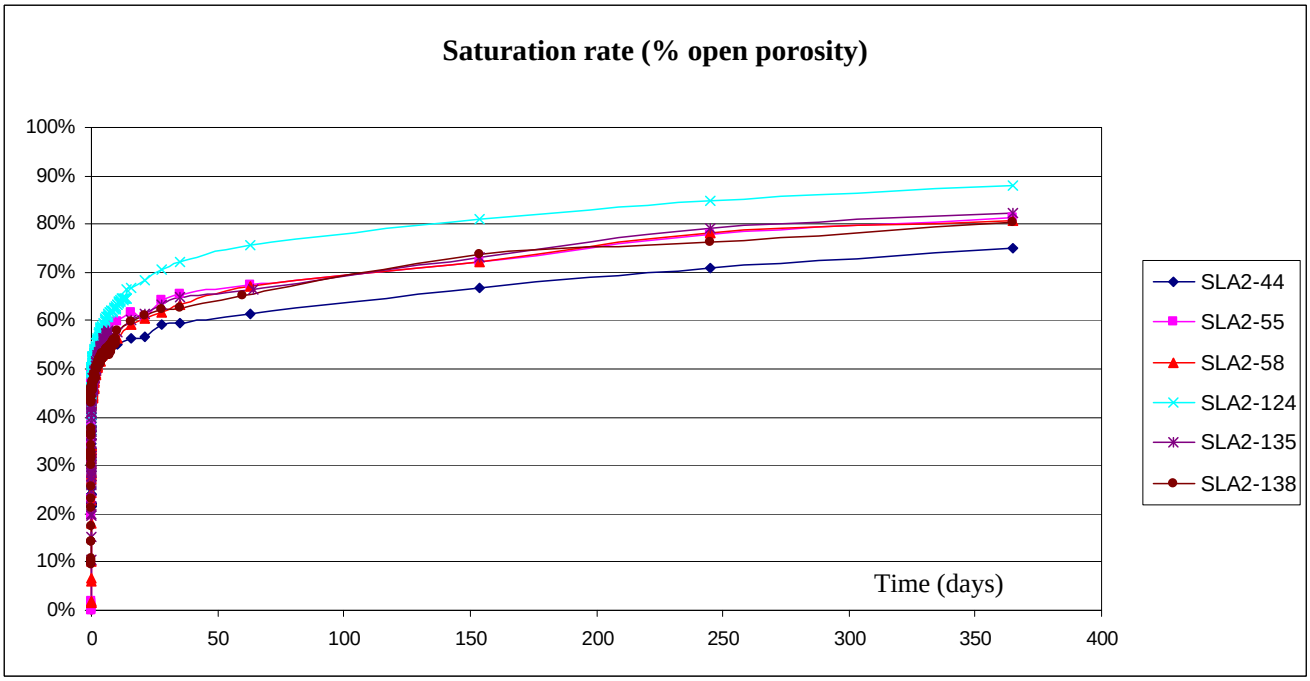


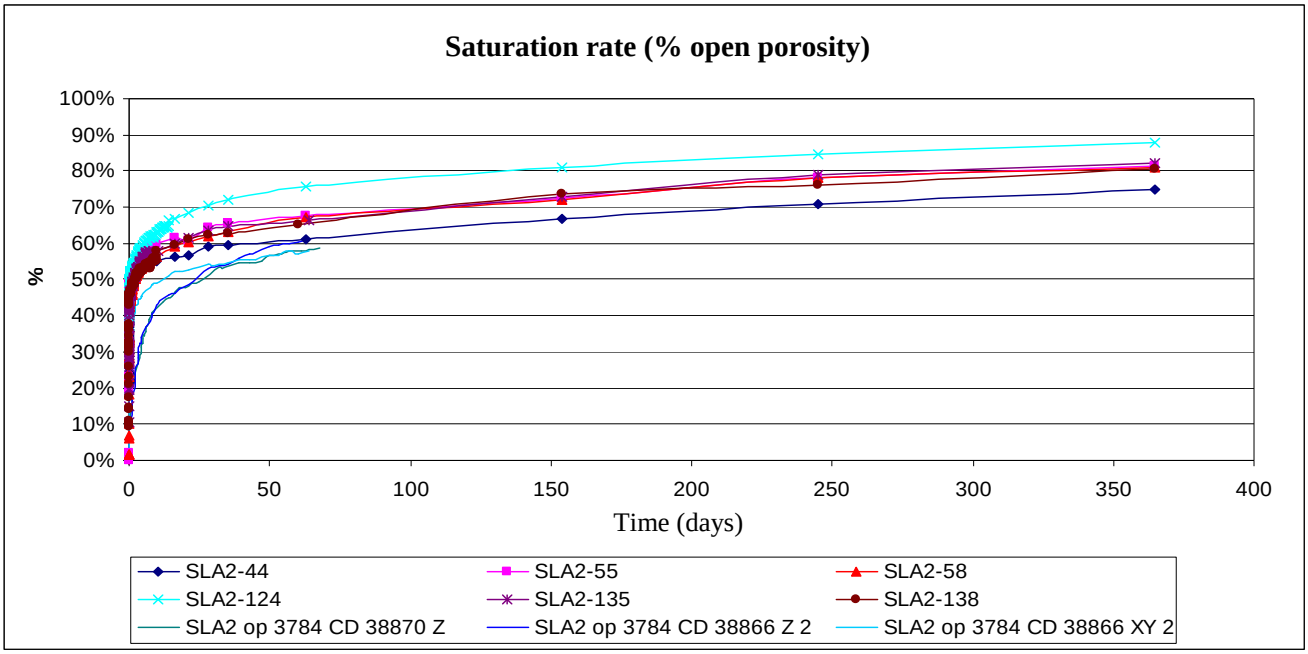
FIGURE 15: Change in irradiated St Laurent A2 sample masses and in the saturation rate

Considering the uncertainty on the measurement of sample volumes, open porosities and mass gains, the following relative uncertainty was associated with each test:

SLA2-44 : 8.2%	SLA2-55 : 7.7%	SLA2-58 : 8.1%
SLA2-124 :8.3%	SLA2-135 : 12.1%	SLA2-138 :14.8%

1.13. Comparison of tests on St Laurent A2 non irradiated and irradiated graphite samples

Figure 16 compares the saturation rate for non irradiated and irradiated samples as a function of time and the square root of time.



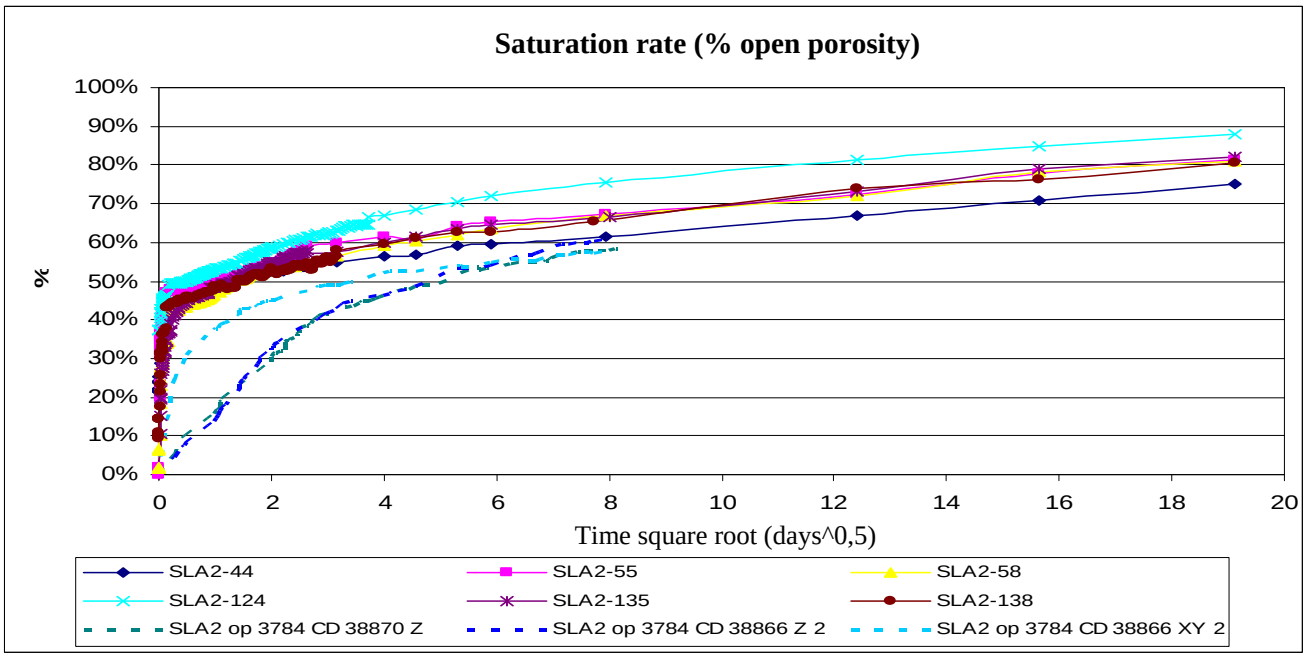


FIGURE 16: COMPARISON OF SATURATION RATES FOR ST LAURENT A2 NON IRRADIATED AND IRRADIATED GRAPHITES MADE FROM LIMA COKE

The results of the irradiated and the non-irradiated samples show a slight difference in their initial mass gain kinetics. The irradiated samples undergo impregnation faster than the non-irradiated samples.
Taking into account the method used to core irradiated samples, they can be compared to the sample taken from the XY plane where the kinetics were faster at the beginning. The figure below shows the variations in the saturation rates over the first 60 days.

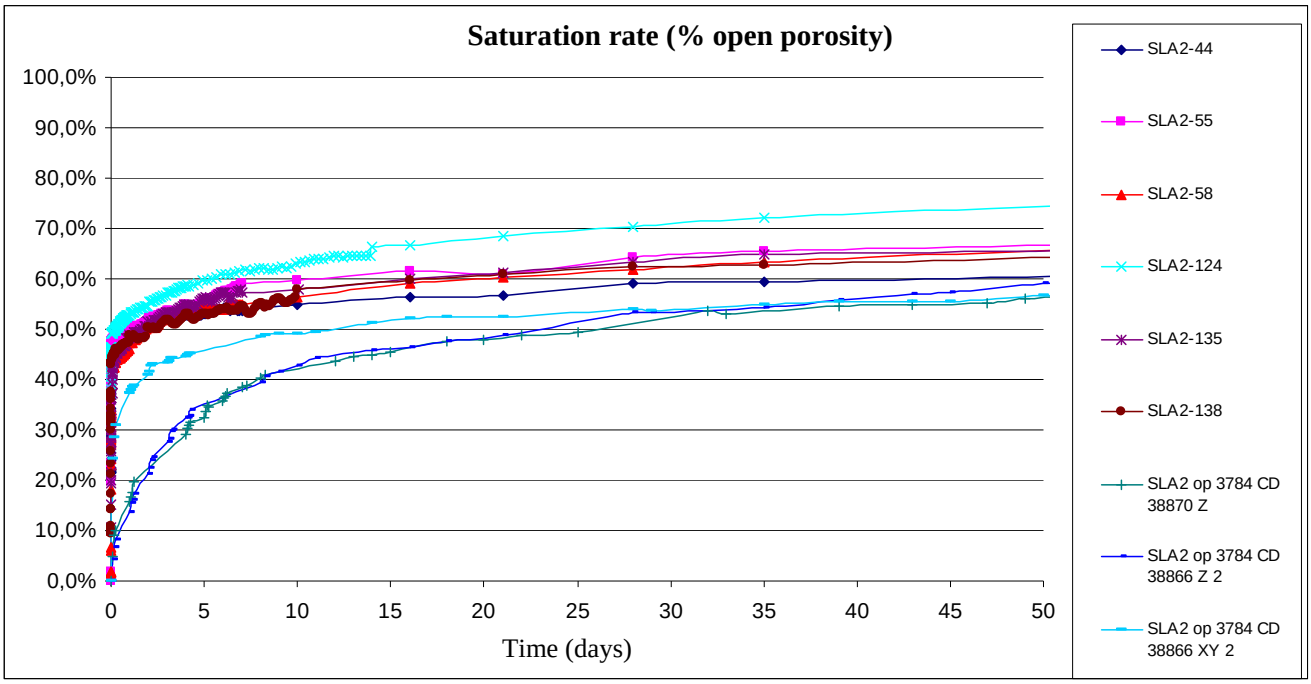


FIGURE 17: COMPARISON OF SATURATION RATES FOR ST LAURENT A2 NON IRRADIATED AND IRRADIATED GRAPHITES MADE FROM LIMA COKE (FIRST DAYS)

Contrary to G2, very little difference can be seen between the saturation rates of non irradiated and irradiated samples from the St Laurent A2 reactor.

DISCUSSION

1.14. Kinetics and impregnation rate of non irradiated samples

It can be seen that the impregnation kinetics of non irradiated graphites differ depending on the origin of the graphite. The following graph compares the impregnation rates over the total duration of the experiments and for the first few days.

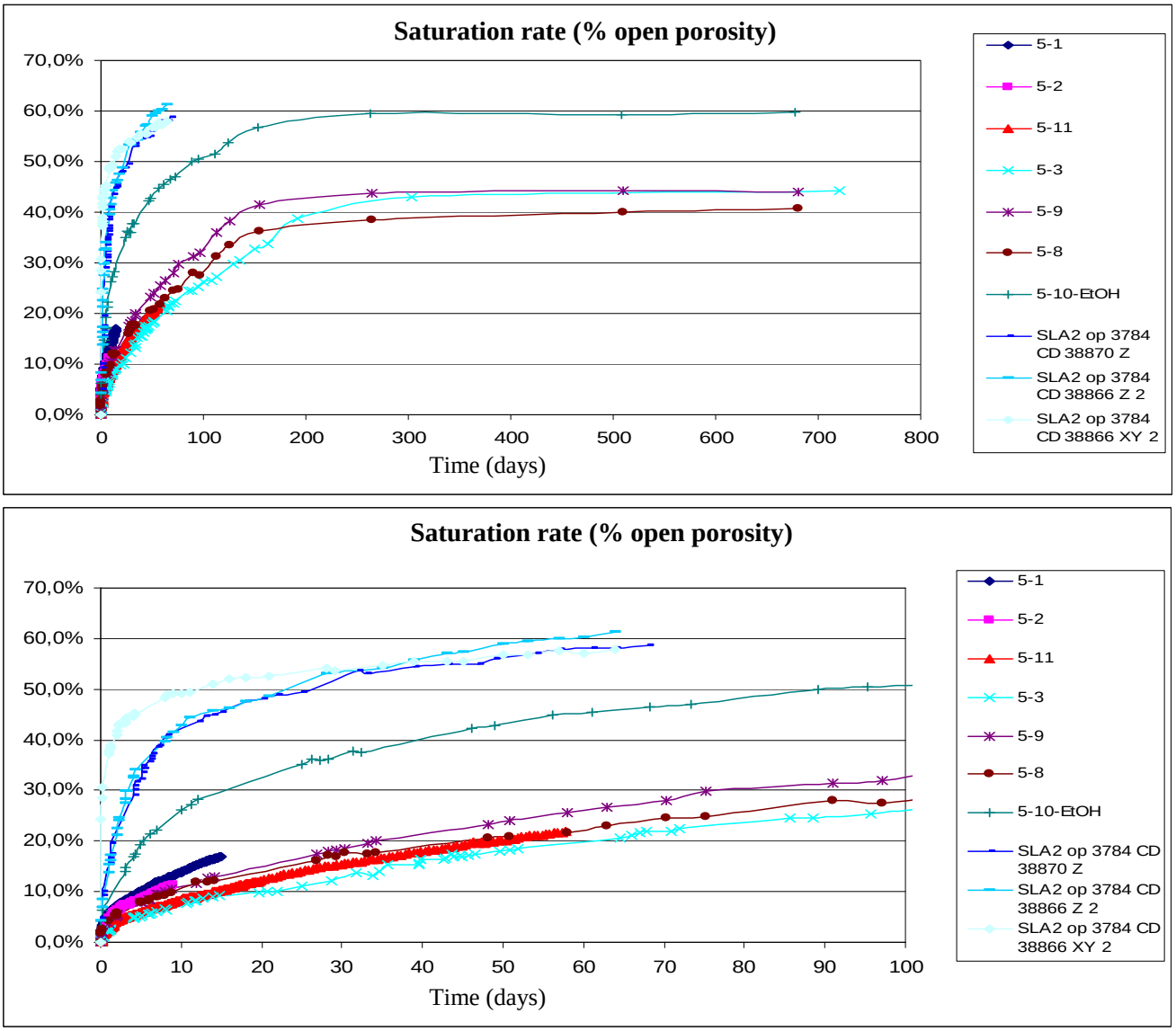


FIGURE 18: COMPARISON OF SATURATION RATES FOR NON-IRRADATED GRAPHITES

Table 20 shows the saturation rates of tests over comparable durations.

Reactor	Test	7 d	14 d	25 d (+/-1)	41 d (+/-1)	113 d	507 d
G2	5-2	9,9%	/	/	/	/	/
G2	5-1	12%	16%	/	/	/	/
G2	5-11	7%	10%	14%	18%	/	/
G2	5-3	6%	9%	11%	16%	27%	/
G2	5-8	9%	12%	17%	21%	31%	40%
G2	5-9	10%	13%	17%	23%	36%	44%
G2	**Mean**	**9±2%**	**12±3%**	**17±3%**	**22±3%**	**34±4%**	**42±2%**
G2	EtOH	22%	28%	35%	42%	52%	59%
SLA2-3784	38870-Z	38%	45%	50%	55%		
SLA2-3784	38866Z2	40%	46%	53%	57%		
SLA2-3784	**38866 XY**	**48%**	**51%**	**54%**	**55%**		

TABLE 20: SATURATION RATES AT DIFFERENT PERIODS FOR IMPREGNATION TESTS ON NON IRRADIATED GRAPHITE SAMPLES (G2 AND SLA2)

These results show that the curve distribution obtained over the first days of impregnation is consistent for the six tests on G2 graphite, with a saturation rate of about 9% in a week and 12% in two weeks. Curve inflection starts after 100 days for longer test periods with the saturation rate practically stabilised after 200 days at about 42%.

Water impregnation is fast in non irradiated St Laurent A2 graphites, with high saturation rates being reached from the first day. After about 7 days, the saturation rates reached 39% in samples taken along the Z axis and 48% in the sample from the XY plane. The three tests show comparable saturation rates after 41 days reaching an average of about 56%. The duration of these tests was too short in order to validate an equilibrium state.

The summary of these tests shows that the impregnation kinetics of non irradiated St Laurent A2 and of G2 graphites are different. The position of the samples in relation to the extrusion axis seems to have an impact on the initial water uptake but the samples shown and identical behaviour and saturation rate after this initial phase.

These results reveal a difference in behaviour which may not only be related to the origin of the cokes (special A coke for G2 and LIMA for SLA2), but also to the graphite manufacturing process (impregnation, graphitisation, purification, etc.). Recent studies conducted by the CEA show that the lattice parameters and the non irradiated G2 graphite structure are closer to the reference graphite (highly ordered pyrolytic graphite – HOPG) than those of the St Laurent A2 graphite.

These studies, which used X-ray diffraction (XRD), were also confirmed by Raman microspectrometry. This analysis technique, just like XRD, can be used to study the crystal structure of the material but on a smaller scale. Raman microspectrometry focuses on areas of 2 to 3 μm^2 while XRD covers areas of about 1 cm^2. Furthermore, in addition to analysing the crystal structure of materials, Raman spectroscopy can also provide information on crystal defects in the sample.

The results (Table 21 and Figure 19) show that the lattice parameter, c, increases and thus the space between the graphene planes is smaller for non irradiated G2 graphite (6,72 Å) than for SLA2 (6,74 Å). This tends to indicate that the quality of graphitisation is better in G2 than in SLA2.

	Parameter c (A) (± 0.002)	***Parameter a (A)*** (± 0.002)
Theoretical parameters	6.707	2.461
non-irradiated G2	6.725	2.460
non-irradiated SLA2	6.740	2.462

TABLE 21: X-RAY DIFFRACTION – LATTAICE PARAMETER OF NON IRRADIATED GRAPHITE SAMPLES

The diffractogram below shows a slight shift in the SLA2 line (002) towards the smaller angles of diffraction, which results in a larger c parameter than that for G2.

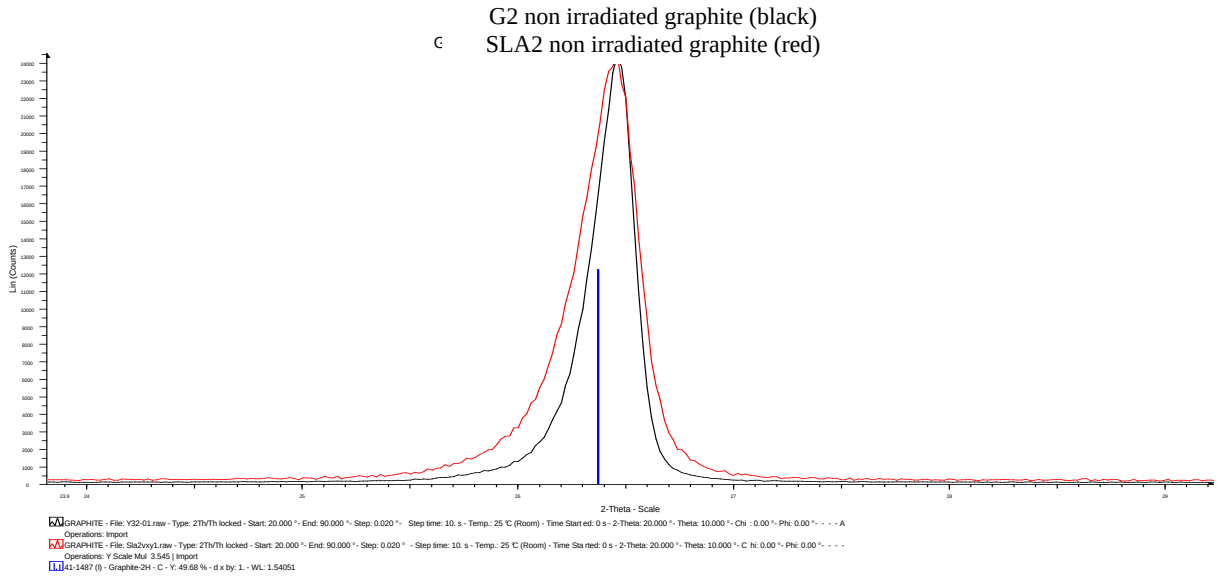


FIGURE 19: DIFFRACTOGRAM OF NON IRRADIATED SLA2 AND G2 GRAPHITE SAMPLES

These defects were also detected during the measurement of defect bands by Raman microscopy as shown in Figure 20, especially defect band D1. Table 22 reports the intensity ratios of the different bands measured on the reference graphites and on the non irradiated G2 and SLA2 graphites.

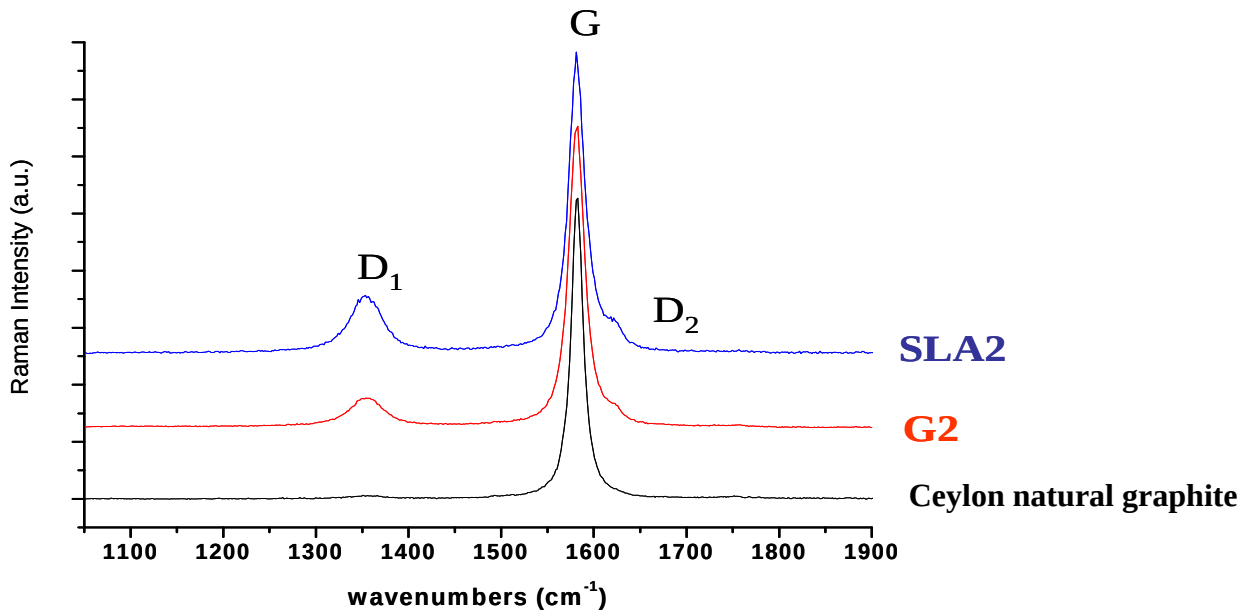


FIGURE 20: RAMAN SPECTRUM OF NON IRRADIATED G2 AND SLA2 GRAPHITE SAMPLES

	FWHMG	$R_1 = \frac{I_{D_1}}{I_G}$	$R_2 = \frac{A_{D_1}}{A_G + A_{D_1} + A_{D_2}}$
Ceylon natural graphite	15.38 ± 1.17	0.009±0.01	0.02 ± 0.02
Non irradiated G2 graphite	19.32 ± 1.87	0.09±0.06	0.15 ±0.07
Non irradiated SLA2 graphite	21.01 ± 1.76	0.18±0.06	0.24±0.06

TABLE 22: CARACTERISTIQICS OF NON IRRADIATED SLA2 AND G2 GRAPHITES BY RAMAN SPECTROSCOPY

FWHMG: Full width at half-maximum of band G
R1: Intensity ratio of the D1 defect band over the G band
R2: Ratio of the defect band D1 area over the sum of the areas

The crystal structure of the G2 graphite is therefore of better quality than that of the SLA2 graphite. The impregnation results (lower impregnation for G2) could therefore be explained by the better-quality graphitisation of the G2 graphite.

1.15. Kinetics and impregnation rate of irradiated samples

The impregnation kinetics of the irradiated samples (except for the G2 reflector sample) are very fast at the beginning: a saturation rate of about 50-70% is reached in several days (Figures 10 and 15). The kinetics then decrease dramatically: the saturation rate increases by about 10% to 20% during a rather long period (200-250 days).

This behaviour can be associated with the pore distribution in the samples which is mainly macroporosity with about 75% to 85% of pore sizes ranging between 1 and 30 µm:

- Impregnation of the macroporosity occurs very quickly in a few days,
- Impregnation of the microporosity - with pore sizes under 1 µm - is slower.

A representation of the saturation rate expressed as a square root of time shows a linear change, which suggests microporosity impregnation is controlled by a diffusion process.

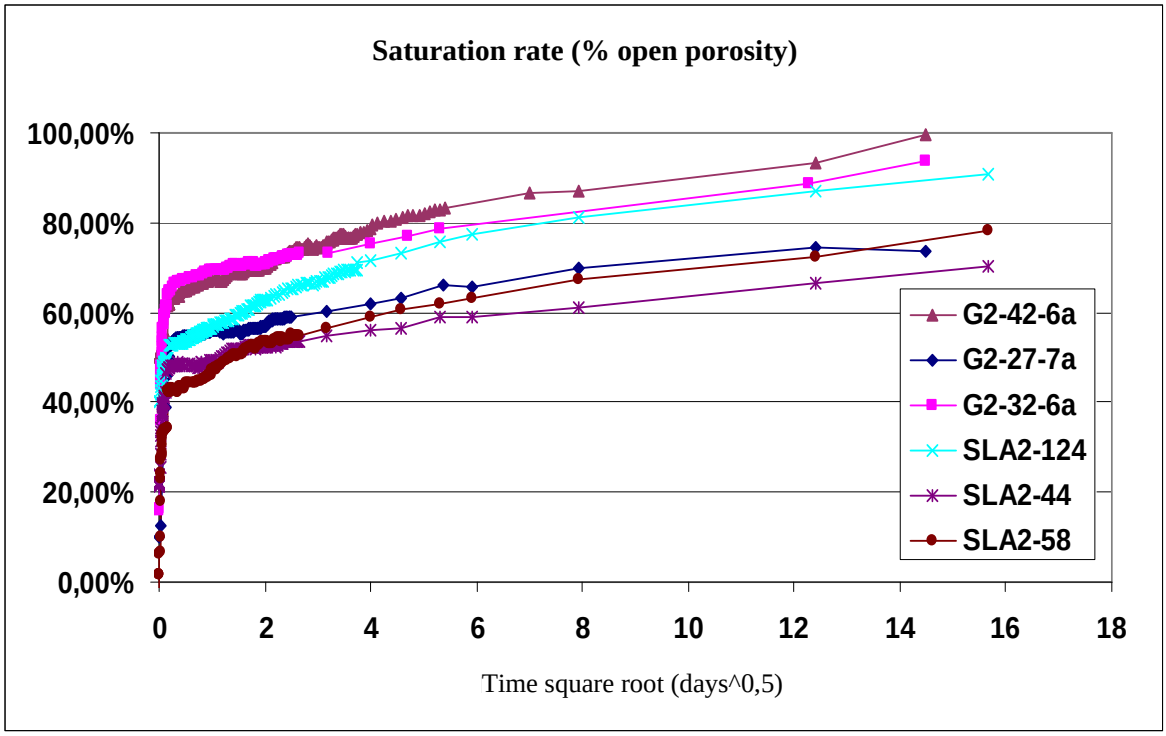
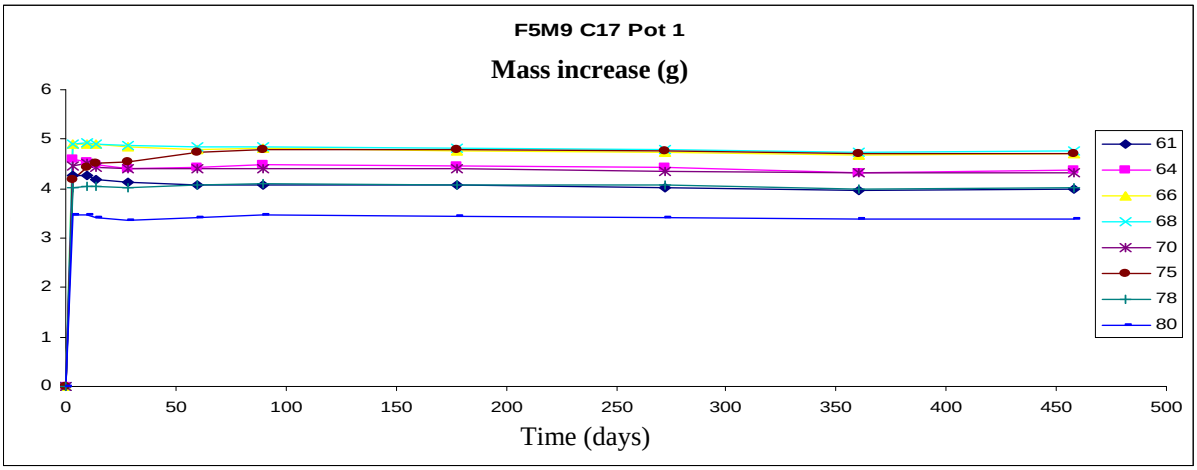
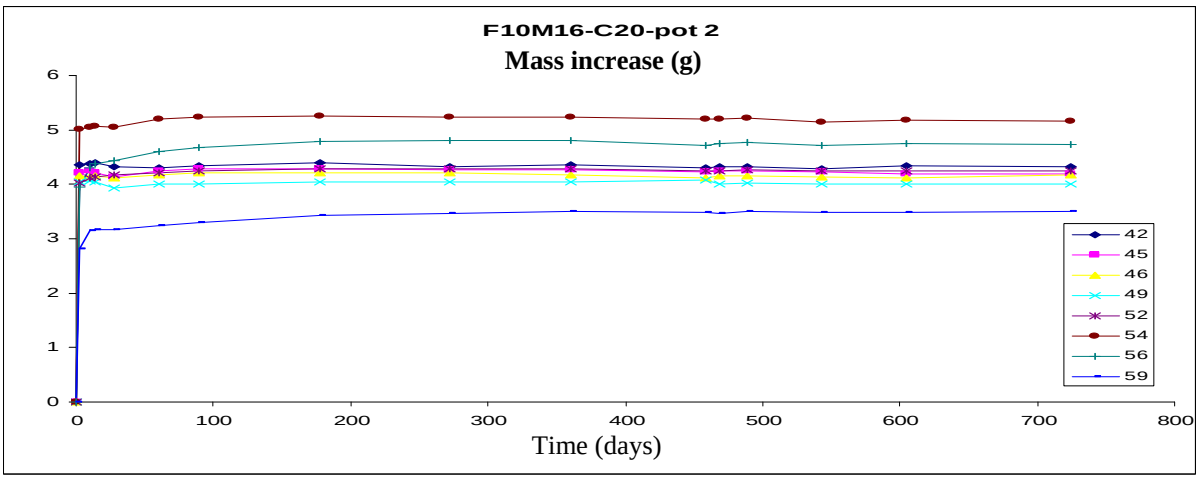


FIGURE 21: CHANGE IN THE SATURATION RATE EXPRESSED AS A SQUARE ROOT OF TIME

Impregnation of the smallest pores may also be controlled by the dissolution of air bubbles trapped in the microporosity. None of these tests were placed in vacuum conditions. Data collected from other St Laurent A2 samples as part of an underwater dismantling study confirmed this assumption. Setting the samples in a vacuum at the beginning of the test results in a faster progression towards the maximum saturation rate (Figure 22).

The graphite samples were first prepared so that only the channel- and brick-facing sides were in contact with water. The samples were also grouped into three batches (pot 1 to 3). The mass gain kinetics of each sample are shown in the following figures. Samples from pots 2 and 3 were taken from the same sampling channel as those studied above. The mass gain, the saturation rate in relation to the open porosity, and the saturation rate in relation to the total porosity are listed in Table 23.





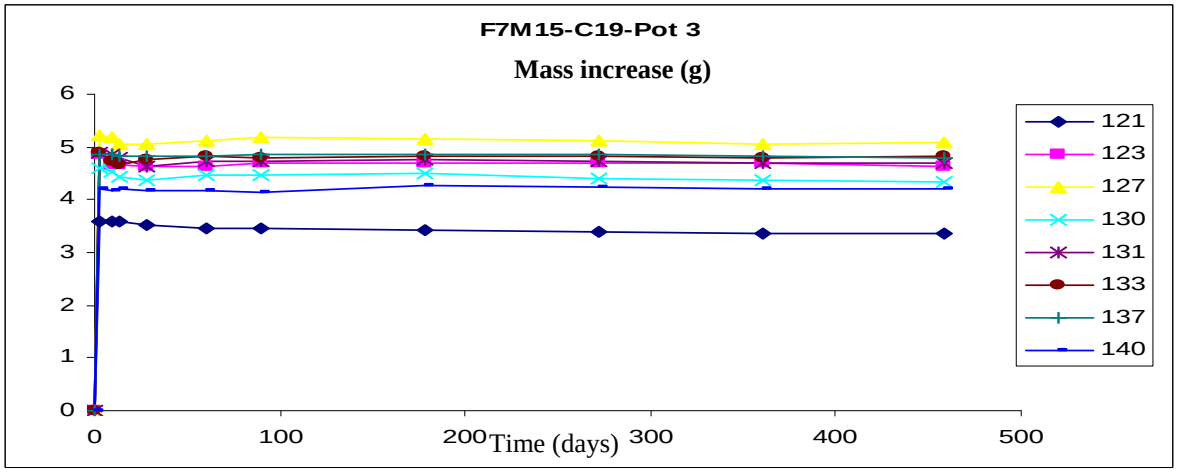


FIGURE 22: CHANGE IN THE MASS OF ST LAURENT A2 SAMPLES FIRST PLACED IN VACUUM CONDITIONS

POT	Sample No.	Channel	Well	Height (mm)	Geometric density	Total porosity	Mass gain (%)	Saturation rate Total porosity	Saturation rate Open porosity
1	SLA2-61	F5 M7	C17	300	1.61±0.08	29.2±1.4%	13%	71±5%	82±6%
1	SLA2-64	F5 M7	C17	2070	1.56±0.08	31.2±1.7%	16%	78±6%	90±7%
1	SLA2-66	F5 M7	C17	3060	1.50±0.08	33.7±1.9%	17%	77±6%	88±7%
1	SLA2-68	F5 M7	C17	3840	**1.47±0.06**	35.2±1.4%	18%	74±4%	**84±5%**
1	SLA2-70	F5 M7	C17	5120	**1.41±0.03**	37.8±0.7%	17%	62±2%	**69±2%**
1	SLA2-75	F5 M7	C17	7280	**1.47±0.07**	35.1±1.7%	16%	69±5%	**78±5%**
1	SLA2-78	F5 M7	C17	8660	**1.41±0.07**	37.9±1.8%	15%	57±4%	**64±4%**
1	SLA2-80	F5 M7	C17	9260	**1.47±0.06**	35.0±1.5%	12%	52±3%	**58±4%**
2	SLA2-42	F10 M16	C20	1080	1.60±0.09	29.6±1.7%	15%	**80±7%**	**92±8%**
2	SLA2-45	F10 M16	C20	2460	1.60±0.10	29.5±1.8%	14%	**75±6%**	**87±7%**
2	SLA2-46	F10 M16	C20	3060	1.54±0.03	32.0±0.6%	14%	**65±2%**	**75±2%**
2	SLA2-49	F10 M16	C20	4480	1.63±0.03	28.0±0.5%	14%	**84±2%**	**98±2%**
2	SLA2-52	F10 M16	C20	5900	1.59±0.03	30.0±0.7%	16%	**86±3%**	**99±3%**
2	SLA2-54	F10 M16	C20	6890	1.45±0.09	36.0±2.3%	20%	**81±7%**	**91±8%**
2	SLA2-56	F10 M16	C20	7880	1.56±0.07	31.1±1.4%	16%	**83±5%**	**95±6%**
2	SLA2-59	F10 M16	C20	9260	1.67±0.08	26.4±1.2%	11%	**72±5%**	**85±5%**
3	SLA2-121	F7 M15	C19	300	1.66±0.06	26.7±1.0%	11%	67±3%	79±4%
3	SLA2-123	F7 M15	C19	1680	1.58±0.07	30.2±1.3%	16%	82±5%	94±6%
3	SLA2-127	F7 M15	C19	3450	1.56±0.07	31.4±1.4%	17%	83±5%	95±6%
3	SLA2-130	F7 M15	C19	5120	1.64±0.03	27.5±0.5%	15%	90±2%	105±3%
3	SLA2-131	F7 M15	C19	5510	1.53±0.03	32.4±0.5%	16%	76±2%	86±2%
3	SLA2-133	F7 M15	C19	6500	1.61±0.07	29.2±1.4%	16%	89±6%	104±7%
3	SLA2-137	F7 M15	C19	8270	1.49±0.04	34.4±1.0%	18%	78±3%	88±4%
3	SLA2-140	F7 M15	C19	9260	1.64±0.07	27.8±1.2%	15%	86±5%	101±6%

TABLE 23: WATER IMPREGNATION IN IRRADIATED SLA2 SAMPLES (MASS GAIN AND MAXIMUM SATURATION RATE – TESTS IN DISMANTLING CONDITIONS)

Case of channel F10M16-C20

Sample No.	Sampling height (mm)	Mass gain (%)	Saturation rate Total porosity	Saturation rate Open porosity	Conditions
SLA2-42	**1080**	**15%**	80±7%	92±8%	1
SLA2-44	**2070**	**11.7**±0.1**%**	65±3	75±6	2
SLA2-45	**2460**	**14%**	75±6%	87±7%	1
SLA2-46	**3060**	**14%**	65±2%	75±2%	1
SLA2-49	**4480**	**14%**	84±2%	98±2%	1
SLA2-52	**5900**	**16%**	86±3%	99±3%	1
SLA2-54	**6890**	**20%**	81±7%	91±8%	1
SLA2-55	**7280**	12.4±0.1	70±3	81±6	2
SLA2-56	**7880**	**16%**	83±5%	95±6%	1
SLA2-58	**8660**	10.6±0.1	68±3	81±6	2
SLA2-59	**9260**	**11%**	72±5%	85±5%	1

TABLE 24: WATER IMPREGNATION IN IRRADIATED SLA2 SAMPLES: MASS GAIN AND MAXIMUM SATURATION RATE – SAMPLE FROM CHANNEL F10M16-C20

Case of channel F7 M15-C19

Sample No.	Sampling height	Mass gain (%)	Saturation rate Total %	Saturation rate Open porosity	Conditions
SLA2-121	**300**	**11%**	67±3%	79±4%	1
SLA2-123	**1680**	**16%**	82±5%	94±6%	1
SLA2-124	**2070**	**15.6±0.1**	77±4	88±7	2
SLA2-127	**3450**	**17%**	83±5%	95±6%	1
SLA2-130	**5120**	**15%**	90±2%	105±3%	1
SLA2-131	**5510**	**16%**	76±2%	86±2%	1
SLA2-133	**6500**	**16%**	89±6%	104±7%	1
SLA2-135	**7280**	**1.9±0.1**	71±6	82±10	2
SLA2-137	**8270**	**18%**	78±3%	88±4%	1
SLA2-138	**8660**	**13.9±0.1**	70±7	81±11	2
SLA2-140	**9260**	**15%**	86±5%	101±6%	1

TABLE 25: WATER IMPREGNATION IN IRRADIATED SLA2 SAMPLES: MASS GAIN AND MAXIMUM SATURATION RATE – SAMPLE FROM CHANNEL F7M15-C19

Conditions No. 1: UNGG tests, coated samples (leaching by the channel- and brick-facing sides only) after being placed in vacuum conditions.
Conditions No. 2: Tests from this study, samples not coated and not placed in vacuum conditions.

When comparing the results from two experiments on SLA2 graphites, the tests reveal mass gains and saturation rates that are slightly lower than those obtained for graphites having first been placed in vacuum conditions. This tends to confirm that impregnation has not stabilised but continues at a slow rate.

Comparison between St Laurent A2 and G2 irradiated graphite samples is shown in Figure 23 below.

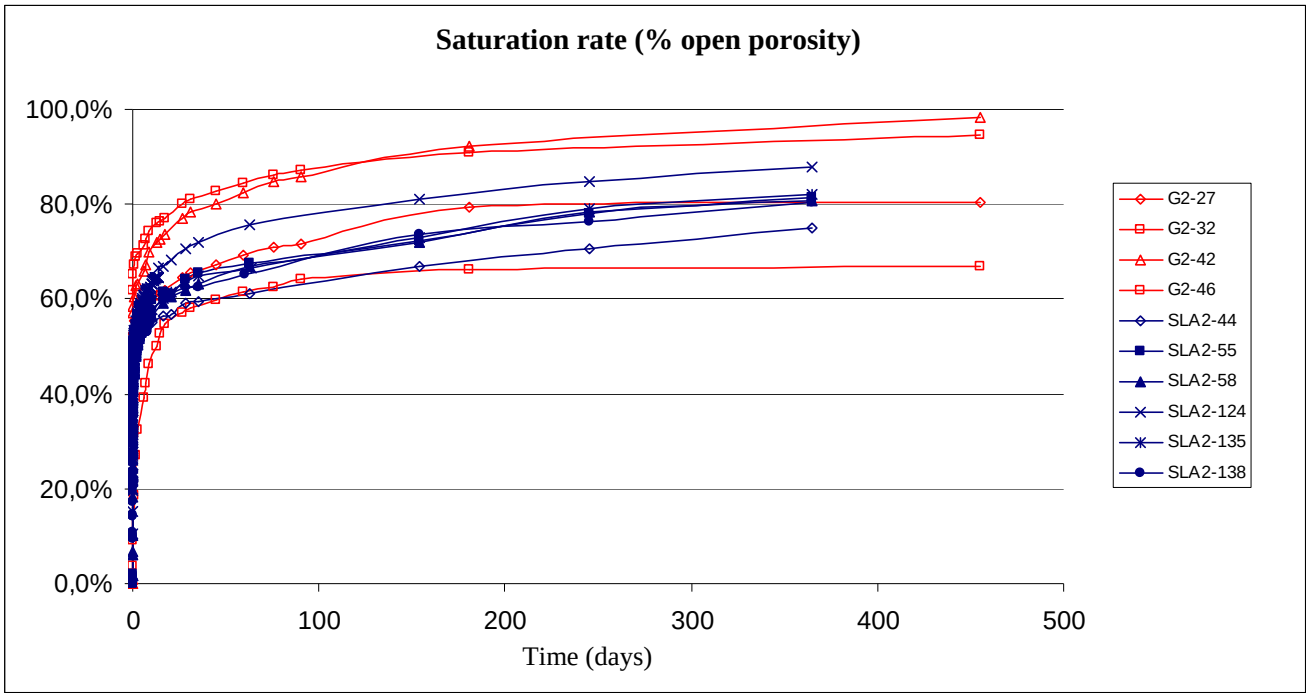


FIGURE 23: COMPARISON OF SATURATION RATES BETWEEN G2 AND SLA2 IRRADIATED SAMPLES

It can be seen that the kinetics are similar and the saturation rates are more or less the same. Irradiation therefore modified the process that governs water impregnation in graphites and tends to homogenise the behaviour of graphites.

When comparing the results of SLA2 samples in greater detail, it can be seen that the variation in the neutron flux – even minor (below a factor of 3) between the different samples – does not seem to have a significant impact on the sample saturation rate.

Comparison of all the results for G2 and SLA2 in relation to the irradiation temperature also proves there is no correlation.

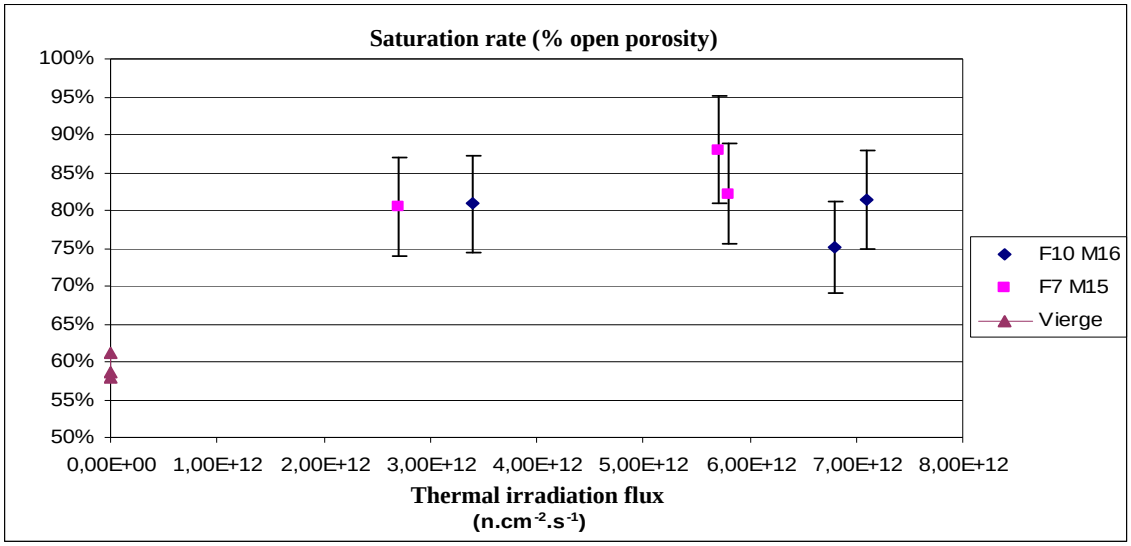


FIGURE 24: CHANGE IN THE SATURATION RATE AS A FUNCTION OF THE THERMAL NEUTRON FLUX (SLA2 SAMPLES)

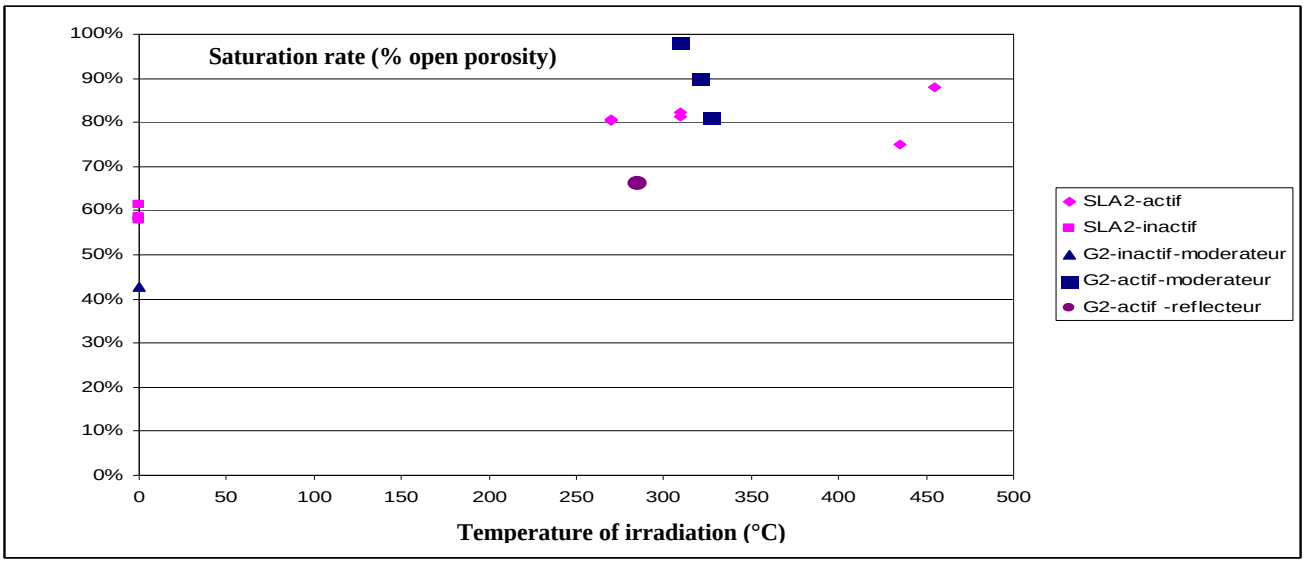


FIGURE 25: CHANGE IN THE SATURATION RATE AS A FUNCTION OF THE IRRADIATION TEMPERATURE (G2 & SLA2 SAMPLES)

The SLA2 graphite data can be supplemented by the test data collected within the scope of dismantling studies, however the increased number of points does not always make it possible to identify a clear correlation between these parameters and the saturation rate of samples.

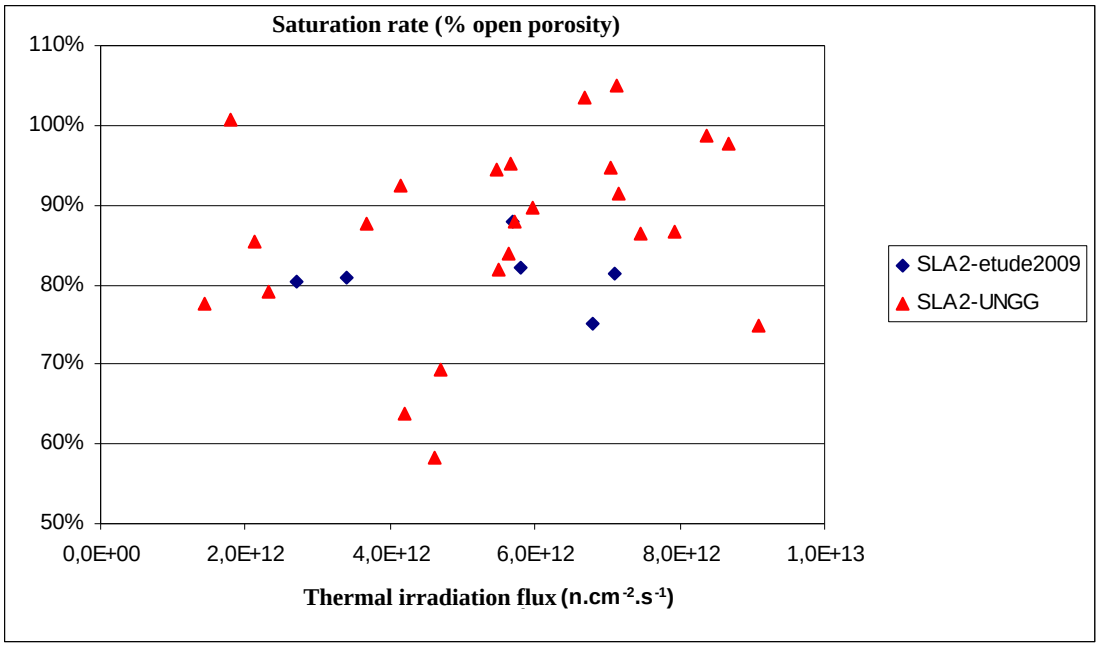


FIGURE 26: CHANGE IN THE SATURATION RATE AS A FUNCTION OF THE THERMAL NEUTRON FLUX FOR SLA2 TESTS

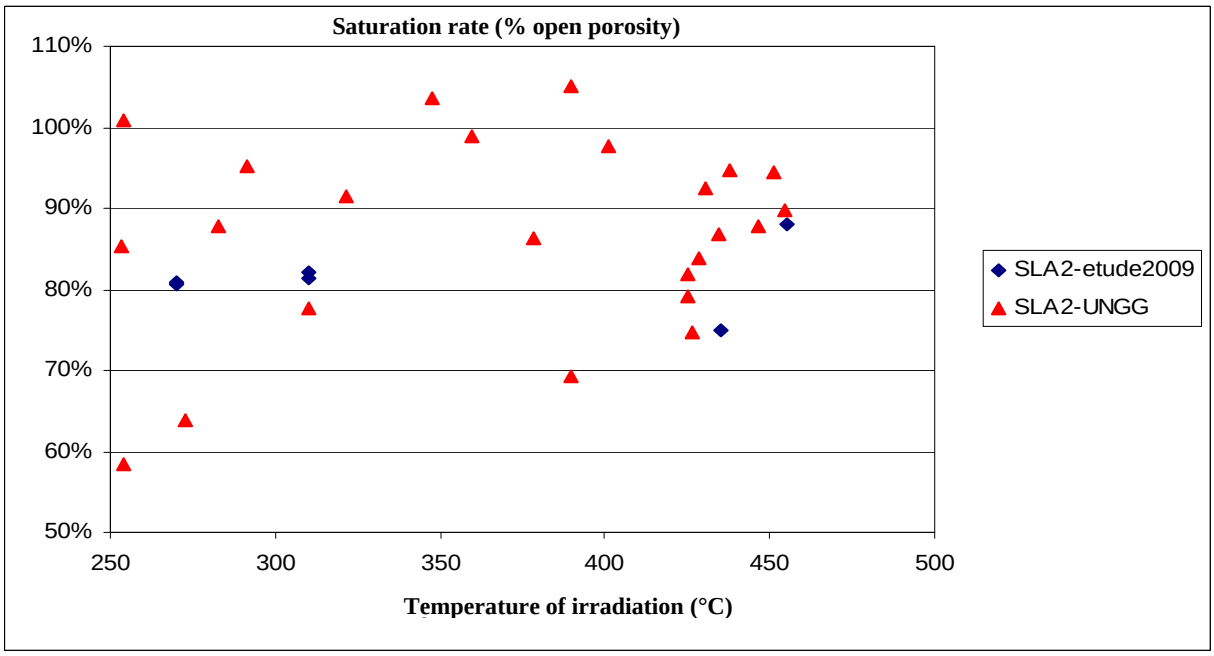


FIGURE 27: CHANGE IN THE SATURATION RATE AS A FUNCTION OF THE IRRADIATION TEMPERATURE (SLA2 SAMPLES)

1.16. Summary

This study reveals the effect of irradiation on the water impregnation of graphites, which tends to increase the impregnation kinetics and the saturation rate of the graphites. The original behaviour of non-irradiated graphites seems to be completely erased by their time in the reactor due to the probable combined effect of the temperature, irradiation and radiolytic corrosion:

- Radiolytic corrosion increases the open porosity. However, the open porosity is only slightly increased (a few percent) whereas the quantity of impregnated water is doubled in irradiated samples. It also modifies the macroporosity of graphites, particularly by widening the mean pore diameter as shown in the mercury intrusion porosimetry spectrums, which may facilitate water impregnation.

- Irradiation and radiolytic corrosion result in breaking the C-C bonds in the graphite crystallites and/or grain boundaries to form more hydrophilic C-H or C-O bonds. This leads to faster and higher impregnation.

- Irradiation combined with temperature modified the crystal structure and especially the lattice parameters. These modifications affect the electrostatic repulsions of graphite, making it more hydrophilic. However, studies conducted jointly by ENS and the CEA/DEN/DMN/SEMI/LPCMI show that the lower the irradiation temperature, the more the crystal structure undergoes modification. Defect rearrangement could be seen in both G2 and SLA2 graphite samples that were subjected to higher temperatures. This thermal effect is not demonstrated in terms of the impregnation rates.

It is not possible to conclude on the effect of each parameter, though the results clearly point to the fast and practically complete impregnation of water in irradiated graphites.

CONCLUSION

Water impregnation in irradiated graphites is the first process that leads to the release of radionuclides contained in the graphite. If this phase is slow and low, it can control both the kinetics and the release rate of radionuclides in solution.

Impregnation tests were therefore performed on non irradiated and irradiated graphite samples from G2 and St Laurent A2 which had been previously characterised by geometric density measurements, He pycnometry, Hg porosimetry, X-ray diffraction and Raman spectroscopy [2]. The porosity and pore distribution of these samples were also determined.

The impregnation results show that irradiation significantly increases the water impregnation kinetics and the saturation rate of G2 St Laurent A2 graphites.

This data will be compared with the radionuclide release kinetics so as to demonstrate whether water impregnation is a phenomenon that limits the leaching of the most mobile radionuclides, particularly ^{36}Cl.

LIST OF TABLES

TABLE 1: CHARACTERISTICS OF G2 AND SLA2 REACTORS

TABLE 2: CHARACTERISATION OF SAMPLES

TABLE 3: IMPREGNATION RATE OF EDF FUEL SLEEVE SAMPLES

TABLE 4: MASS GAIN PERCENTAGES OF IRRAIDATED AND NON-IRRADIATED GRAPHITE SAMPLES

TABLE 5: MASS GAIN OF IRRADIATED GRAPHITE BLOCKS DURING LEACHING

TABLE 6: WATER RETENTION IN HANFORD GRAPHITES DURING LEACHING TESTS

TABLE 7: CHARACTERISTICS OF FRESH G2 SAMPLES FOLLOWIN WATER IMPREGNATION

TABLE 8: CHARACTERISTICS OF FRESH G2 SAMPLE AFTER IMPREGNATION IN A MIXTURE OF WATER AND ETHANOL (10 WT%)

TABLE 9: G2 SAMPLES CHOSEN FOR LEACHING TESTS

TABLE 10: CHARACTERISTICS OF SAMPLES – G2 CUBE

TABLE 11: CHARACTERISTICS OF SAMPLES – G2 CYLINDER

TABLE 12: SURFACE TENSION AT 20℃

TABLE 13: WATER IMPREGNATION IN IRRADIATED G2 SAMPLES (MASS GAIN AND MAXIMUM SATURATION RATE)

TABLE 14: CHARACTERISTICS OF NON-IRRADIATED SLA2 SAMPLES

TABLE 15: SLA2 GRAPHITE SAMPLES CHOSEN FOR THE LEACHING TESTS

TABLE 16: CHARACTERISTICS OF SLA2 IRRADIATED SAMPLES

TABLE 17: POROSITY AND DENSITY OF SAMPLES FROM CHANNEL F10M10-C20 [11]

TABLE 18: EXTRACT OF DATA FOR SAMPLES FROM CHANNEL F5M19-C20 [12]

TABLE 19: WATER IMPREGNATION IN IRRADIATED SLA2 SAMPLES (MASS GAIN AND MAXIMUM SATURATION RATE)

TABLE 20: SATURATION RATES AT DIFFERENT PERIODS FOR IMPREGNATION TESTS ON FRESH GRAPHITE SAMPLES (G2 AND SLA2)

TABLE 21: X-RAY DIFFRACTION – LATTAICE PARAMETER OF FRESH GRAPHITE SAMPLES

TABLE 22: CARACTERISTIQICS OF FRESH SLA2 AND G2 GRAPHITES BY RAMAN SPECTROSCOPY

TABLE 23: WATER IMPREGNATION IN IRRADIATED SLA2 SAMPLES (MASS GAIN AND MAXIMUM SATURATION RATE – TESTS IN DISMANTLING CONDITIONS)

TABLE 24: WATER IMPREGNATION IN IRRADIATED SLA2 SAMPLES: MASS GAIN AND MAXIMUM SATURATION RATE

– SAMPLE FROM CHANNEL F10M16-C20

TABLE 25: WATER IMPREGNATION IN IRRADIATED SLA2 SAMPLES: MASS GAIN AND MAXIMUM SATURATION RATE – SAMPLE FROM CHANNEL F7M15-C19

LIST OF FIGURES

FIGURE 1: VARIATION IN THE QUANTITY OF WATER ADSORBED IN THE GRAPHITE SAMPLES 8
FIGURE 2: CORRECTED IMPREGNATION RATES OF THE V/S RATIO 9
FIGURE 3: IMPREGNATION RATE VARIATIONS FOR THE ENTIRE FUEL SLEEVE USING THE SQUARE-ROOT-OF-TIME RULE 9
FIGURE 4: SATURATION RATE OF NON IRRADIATED SAMPLES FROM THE G2 AND B REACTORS..... 10
FIGURE 5: EFFECT OF RADIOLYTIC CORROSION ON THE SATURATION RATE 11
FIGURE 6: CROSS-SECTIONS OF THE NON-IRRADIATED G2 GRAPHITE BRICK 15
FIGURE 7: REPRESENTATION OF G2 REACTOR WITH VERTICAL CORING AND LOCATION OF CORE SAMPLES..... 16
FIGURE 8: CHANGE IN NON IRRADIATED G2 SAMPLE MASSES AND THE SATURATION RATE 19
FIGURE 9: CHANGE IN THE MASS OF IRRADIATED G2 SAMPLES (CYLINDER (A) AND CUBE (B))..... 20
FIGURE 10: SATURATION RATE OF IRRADIATED G2 SAMPLES (CYLINDER (A) AND CUBE (B)) 21
FIGURE 11: COMPARISON OF SATURATION RATES FOR G2 NON IRRADIATED AND IRRADIATED GRAPHITE SAMPLES MADE FROM SPECIAL A COKE (MODERATOR)..... 23
FIGURE 12: SLA2 GRAPHITE CORE AND ITS DISTRIBUTION FOR THE DIFFERENT ANALYSES 25
FIGURE 13: CHANGE IN NON IRRADIATED ST LAURENT A2 SAMPLE MASSES AND THE SATURATION RATE 28
FIGURE 14: LOCATION OF SAMPLES TAKEN FROM THE ST LAURENT A2 REACTOR IN RELATION TO THE SAMPLING PLANE..... 29
FIGURE 15: CHANGE IN IRRADIATED ST LAURENT A2 SAMPLE MASSES AND IN THE SATURATION RATE 31
FIGURE 16: COMPARISON OF SATURATION RATES FOR ST LAURENT A2 NON IRRADIATED AND IRRADIATED GRAPHITES MADE FROM LIMA COKE..... 32
FIGURE 17: COMPARISON OF SATURATION RATES FOR ST LAURENT A2 NON IRRADIATED AND IRRADIATED GRAPHITES MADE FROM LIMA COKE (FIRST DAYS) 33
FIGURE 18: COMPARISON OF SATURATION RATES FOR NON-IRRADATED GRAPHITES 34
FIGURE 19: DIFFRACTOGRAM OF NON IRRADIATED SLA2 AND G2 GRAPHITE SAMPLES..... 37
FIGURE 20: RAMAN SPECTRUM OF NON IRRADIATED G2 AND SLA2 GRAPHITE SAMPLES..... 37
FIGURE 21: CHANGE IN THE SATURATION RATE EXPRESSED AS A SQUARE ROOT OF TIME 39
FIGURE 22: CHANGE IN THE MASS OF ST LAURENT A2 SAMPLES FIRST PLACED IN VACUUM CONDITIONS 40
FIGURE 23: COMPARISON OF SATURATION RATES BETWEEN G2 AND SLA2 IRRADIATED SAMPLES..... 43
FIGURE 24: CHANGE IN THE SATURATION RATE AS A FUNCTION OF THE THERMAL NEUTRON FLUX (SLA2 SAMPLES)..... 44
FIGURE 25: CHANGE IN THE SATURATION RATE AS A FUNCTION OF THE IRRADIATION TEMPERATURE (G2 & SLA2 SAMPLES)..... 44
FIGURE 26: CHANGE IN THE SATURATION RATE AS A FUNCTION OF THE THERMAL NEUTRON FLUX FOR SLA2 TESTS 45
FIGURE 27: CHANGE IN THE SATURATION RATE AS A FUNCTION OF THE IRRADIATION TEMPERATURE (SLA2 SAMPLES)..... 45

REFERENCES

[*1*] Comportement des radionucléides dans les graphites UNGG en milieu aqueux / Synthèse bibliographique et proposition de programme. NT SA3C/LARC 08/02. C. Pichon.

[*2*] Caractérisation des graphites des empilements G2 avant et après irradiation. NT SA3C/LARC 09/08.

[*3*] Recherche de données expérimentales sur l'adsorption et la désorption de l'eau par le graphite (déchets UNGG).

[*4*] Rétention d'eau par du graphite irradié. S. Fillet.

[*5*] Conditionnement pour le stockage définitif des briques de graphite radioactif provenant du déclassement des réacteurs. J.R. Costes, Ch. Koch, C. de Tassigny, H. Vidal, A. Raymond. Commission des communautés européennes, EUR 12815 FR, 1990.

[*6*] Conditioning of graphite bricks from dismantled gas-cooled reactors for disposal. J.R. Costes, C. de Tassigny, H. Vidal. Waste Management, Vol. 10, p 297-302, 1990.

[*7*] « Assessment of management modes for graphite from reactor decommissioning » Nuclear science and technology, CEE EUR 9232

[*8*] Report following the agreement for the exchange of irradiated graphite sample and leaching data between the united states department of energy and the commissariat à l'Energie Atomique, JR Costes, H.Vidal , A Raymond and D. Rémy, UDIN/EAp 92/223 – 1992

[*9*] Lixiviation des empilements Graphite de G2 - Comportement des radionucléides (^{36}Cl, ^{14}C, ^{3}H, …) NT SA3C/LARC NT 07-02, C. Guy, J.Comte, 2007

[10] Répartition de température dans l'empilement de graphite des piles G2 et G3 en fonctionnement normal » A l'Homme –F Mauracq.

[*11*] Caractérisation du graphite du réacteur St Laurent A2. DMN/SEMI/LM2E/NT/2006-12A JP Bonal et col. 2006

[*12*] Graphite des empilements des réacteurs UNGG : Chinon A3,Bugey 1,Saint Laurent A2. Synthèse des mesures des propriétés mécaniques et de dégazage –état d'avancement 2006. CEA/CAD/DGI/SEEC/LECD R3 NT352 – S. Parraud -